HYDROLOGIC MODELING OF CONVENTIONAL AND CONSERVATION FARMING PRACTICES ON THE PALOUSE

By

JOSHUA BERNARD VAN WIE

A thesis submitted in partial fulfillment of
the requirements for the degree of

MASTER OF SCIENCE IN CIVIL ENGINEERING

WASHINGTON STATE UNIVERSITY
Department of Civil and Environmental Engineering

AUGUST 2010

To the Faculty of Washington State University:

The members of the Committee appointed to examine the thesis of JOSHUA BERNARD VAN WIE find it satisfactory and recommend that it be accepted.

_____

Jennifer C. Adam, Ph.D., Chair

_____

Michael E. Barber, Ph.D

_____

Jeffrey L. Ullman, Ph.D

HYDROLOGIC MODELING OF CONVENTIONAL AND CONSERVATION

FARMING PRACTICES ON THE PALOUSE

ABSTRACT

by Joshua Bernard Van Wie, M.S.
Washington State University
August 2010

Chair: Jennifer C. Adam

The production of dryland crops, such as spring and winter wheat, in a semi-arid region requires a reliable and adequate water supply. This supply of water available for crop use is of heightened importance in areas such as the Palouse region where the majority of annual rainfall occurs during the winter months and must be retained in the soil through the dry summer growing season. Farmers can increase water conservation at the field and watershed scales through the adoption of best management practices that incorporate tillage practices and crop residue management.

This research analyzed conventional tillage (CT) and no-till (NT) cropping practices by representing them in a watershed-scale hydrologic model in order to determine whether either practice would effectively increase water storage prior to the growing season. The Distributed Hydrology Soil Vegetation Model (DHSVM) was applied and calibrated to represent the physical changes to infiltration, evaporation, and runoff that result from changes in the amount of residual crop cover after harvest brought on by management practices. The model was calibrated with field observations at (1) the basin scale using streamflow observations followed

by (2) the field scale using runoff observations from individual plots that are under CT and NT management.

DHSVM was calibrated to produce a Nash-Sutcliffe (N.S.) model efficiency of 0.69, which falls within the range of efficiencies for DHSVM reported in literature (0.57 – 0.91). By adjusting transmittance factors and albedo for crop residue versus bare ground, the model was modified to incorporate the effects of CT and NT practices on the surface energy balance and infiltration and runoff on frozen soil. DHSVM was found to predict surface temperature with an N.S. efficiency of 0.60, and the model was able to predict the soil state, either frozen or unfrozen, 81% of the time. In order to simulate evaporation dynamics CT was modeled as bare soil while NT is modeled as a dead-vegetation understory.

It was found that modeled soil moisture was approximately 50% lower during the majority of the winter months in CT management than NT. Predicted volumetric soil moisture content on April 1st was 0.29 in conventionally tilled farmland, while no-till farmland had a moisture content of 0.34. This difference in winter and spring soil moisture was caused primarily by decreased evaporation under NT, with minimal effects of decreased infiltration into frozen ground. Two methods of crop yield estimation indicated that the increased spring soil moisture of NT may result a 19% increase in wheat yield.

It was concluded that NT farming has the potential to increase the capture and retention of winter precipitation in the root-zone that may result in higher yields of spring and winter wheat in the Palouse. Furthermore, DHSVM was found to be suitable for investigating regional agricultural management issues and demonstrates the potential to address additional scientific questions pertaining to sustainable farming.

TABLE OF CONTENTS

LIST OF FIGURES

LIST OF TABLES

INTRODUCTION

The agricultural practice of field tillage has dramatic effects on surface hydrologic properties, significantly altering the processes of infiltration, evaporation, and runoff (Jalota et al., 2000; Mizuba and Hammel, 2001; Singh et al., 2009). In dryland farming regions, such as the Palouse region of the Pacific Northwest, it is essential to maintain an adequate and reliable water supply for the sustainable growth of crops. While field studies (Hammel, 1996; McCool et al., 2006) have demonstrated that conservation tillage strategies may have the ability to increase local soil moisture storage, there is a need for a more thorough understanding of the implications of a region-wide shift to conservation farming.

Wheat yields for both winter and spring wheat are limited by the availability of moisture during most years (Chan and Heenan, 1996; Oweis et al., 1999; Pannkuk et al., 1998), and both varieties have high moisture demands during the spring months as spring wheat begins to be established and winter wheat matures. Studies have indicated that the emergence of seedlings is delayed and the percent of seeds that germinate decreases as soil moisture contents decline (Hanks and Thorp, 1956; Noori et al., 1985; Lindstrom et al., 1976). Inagaki et al. (2007) found that early emergence of wheat heads is critical for high yields in dry areas, and Owen (1952) concluded that maximum germination of seeds cannot occur at a water potential of less than 15 bars. Wheat begins to emerge within the first two weeks after being planted (Noori et al., 1985), making the successful growth of spring wheat completely dependent on water stored in the soil during the winter season. Winter wheat also relies on moisture stored over the winter as the dormant plants begin to grow again in the spring. Lack of water during the spring growth

stages of winter wheat has been found to decrease yields (Day and Intalap, 1970; Schillinger et al., 2008), and soil moisture on April 1st has been found to be correlated with wheat yields, having a correlation coefficient of r = 0.77 (Leggett, 1959).

During the winter, the Palouse is characterized by unsteady temperatures that cause fluctuation between rain and snow storms and frequent freezing and thawing of the upper soil layers. A single winter in the Northwest will often experience greater than 100 freeze-thaw cycles (Hershfield, 1974; McCool and Roe, 2005), and large runoff events commonly occur due to a combination of snow melt and rainfall on snow or frozen soil (Pikul et al., 1996; Zuzel et al., 1982). A large portion of precipitation during the cold season contributes to streamflow rather than infiltrating into the soil (Davis and Molnau, 1973) making the capture and storage of winter precipitation crucial for maintaining adequate soil moisture for crop uptake during the summer growing season.

Tillage occurs after harvesting and influences field conditions prior to the winter months. Conventional tillage (CT) that completely overturns the top soil and buries residue has long been established in the United States, but new methods of less intensive cultivation began to gain popularity after being introduced in the mid 1900s (Lal et al., 2007). Conservation methods include a variety of tillage types that leave at least 30% crop residue (Guy et al., 2002) above the ground, the most intensive being no-till farming (NT) in which no tillage is performed, leaving the soil surface completely undisturbed. These conservation techniques are practiced on only 23% of the farmland in Washington State, while 36% of all farmland is under conservation tillage nationwide (CTIC, 2001). Adoption of conservation practices has been slow in the Palouse because of concerns about economic risk and profitability (Juergens et al., 2004)

and many farmers continue to practice systems involving eight or more passes with various tillage implements in certain parts of the region (Schillinger et al., 2007).

Tillage interacts with the water cycle by affecting surface runoff, evaporation, and infiltration. Reduced tillage methods that leave a larger percentage of the crop residue on the surface have the advantage of reducing runoff and increasing infiltration by creating a physical barrier that traps water. In a study performed at a research site near Pullman, WA, Greer et al. (2006) found that 3 conventionally tilled fields produced an average of 66.0 mm runoff over a five-month period while 3 no-till fields produced a negligible amount, averaging only 0.3 mm during the same time span. Similar results have been replicated in various studies, demonstrating that no-till greatly reduces runoff and increases soil moisture in the annual cropping areas of the Palouse (Cochran et al., 1982; Fuentes et al., 2003; McCool et al., 2006; Papendick and McCool, 1996). The residue layer also provides a barrier against evaporation, and tillage practices that increase residue have been found to provide increased resistance to vapor transfer from the soil to the atmosphere (Cornish and Pratley, 1991; Jalota et al., 2000). In addition to providing a physical barrier against runoff and evaporation, crop residue provides an insulating layer that can help regulate soil temperature (Hammel et al., 1981; Vomocil et al., 1984) by decreasing soil heat losses by up to 40% through insulation (Pikul et al., 1986). By increasing winter soil temperature, fields with thicker residue layers experience shallower freezes and fewer runoff events (Dowding et al., 1984).

The objective of this research is to investigate the hydrologic effects of a region-wide adaptation of no-till farming compared with conventional tillage methods. The Distributed Soil Hydrology Vegetation Model (DHSVM; Wigmosta et al., 1994) is applied to specifically examine

the process of soil freezing and resulting changes in hydraulic conductivity and infiltration on two scales: a small field plot and a complete watershed. After calibration at the field scale the model is used to investigate two hypothetical scenarios in the Palouse region: one situation in which land is managed conventionally with intensive tillage and the other representing a region-wide shift to no-till practices. The frequency of soil freezing, runoff, infiltration, and spring soil moisture are compared for the two scenarios. A variety of studies on the interactions between tillage and the water and energy cycles have been performed on individual field plots (Cochran et al., 1982; Fuentes et al., 2003; Hammel et al., 1981; McCool et al., 2006; Papendick and McCool, 1996; Vomocil et al., 1984). Watershed scale examinations have been largely neglected, with only a limited number of studies being found in literature. Notable research on the effects of tillage practices on hydrology at a watershed scale include assessment of corn farming in the Midwest (Tomer et al., 2008; Tomer et al., 2006). However, no known work exists that expands upon field studies of wheat farming in the Pacific Northwest to understand the degree to which the regional water balance is influenced by tillage. It is necessary to quantify the widespread impacts of tillage in order to continue to make well informed management decisions that will guide the future of productivity and sustainable farming in the Palouse region.

MATERIALS AND METHODS

1. Study area

The semi-arid climate of the Palouse (a region of predominantly dryland agriculture) makes the availability of water a limiting factor for crop establishment and growth. The region receives an average of 500 mm precipitation annually (PRISM Group, 2009; Daly et al., 1994), of which approximately 70% occurs between November and April, causing the dry summer months to coincide with the period in which crops are maturing and crop water demand is highest. Specific cropping practices in the Palouse vary according to the amount of rainfall received in a particular area. The western portion of the region receives less than 250 mm of rainfall annually, making it necessary for farmers to harvest crops once every two years, leaving the fields fallow during the alternate years to reestablish soil moisture. Annual cropping is practiced in the eastern portion of the Palouse that receives above 450 mm annual precipitation. Winter and spring wheat are the predominant crops grown in both the crop/fallow region and the annual cropping region.

The study was conducted in the upper section of the Palouse River basin (shown in Figure 1), which includes the North and South Forks of the Palouse River and overlaps the border of Washington and Idaho, covering an area of 2000 km^2 and ranging in elevation from 600 to 1600 m. Land cover in the upper Palouse basin is primarily agricultural with forest covering approximately one quarter of the area in the Northeast section of the watershed. Urban concentrations exist in the cities of Moscow and Pullman and in a few smaller rural towns. An average of 531 mm rainfall is received in the watershed (PRISM Group, 2009),

providing enough moisture for crops to be grown and harvested annually without the need for a fallow season to replenish soil moisture. Soil in the basin is Palouse silt loam (USDA-NRCS, 2009).

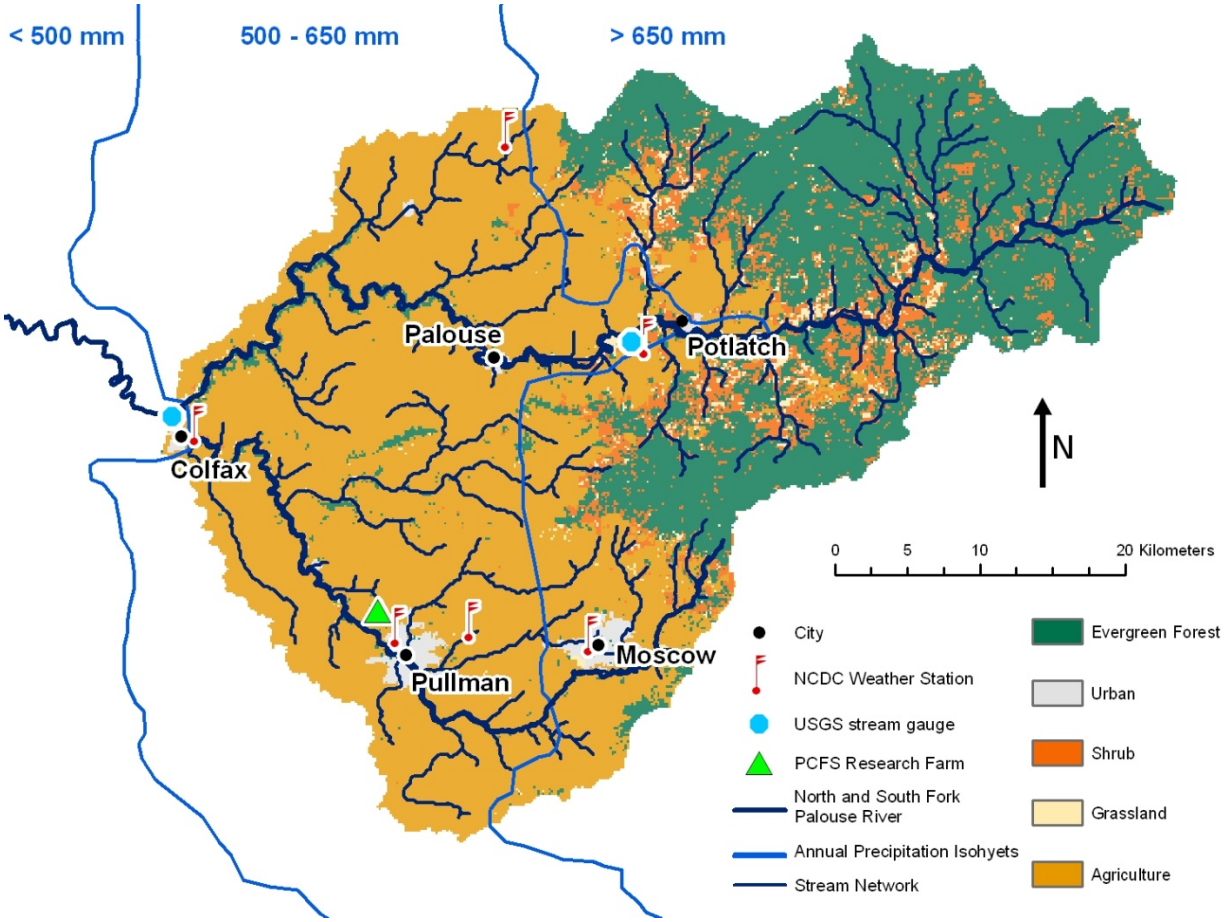

Figure 1. Upper Palouse River basin containing the North and South forks of the Palouse River, which were both used in model calibration. Average annual precipitation isohyets (PRISM group, 2009) are shown along with NLCD land cover data (Homer et al., 2001)

2. Field monitoring

The Palouse Conservation Field Station (PCFS) is located north of Pullman, WA at 46°44'*N*, 117°8'*W* and an elevation of 762 m above sea level (see Figure 1). The site has been used for diverse field studies and testing of conservation technologies including research on conservation tillage techniques (Greer et al., 2006; McCool et al., 2006; Singh et al., 2009). This study used results from the site published by Singh et al. (2009) for field scale DHSVM calibration. Singh et al. conducted a study on the PCFS in which CT and NT were applied to three sets of paired winter wheat plots. CT plots were tilled three times and left bare through the entire winter and NT plots were seeded with winter wheat directly into the existing wheat stubble. Tillage and planting occurred in September of each year. Each plot was 24 m long by 3.7 m wide and plot slopes were 17, 23, and 24%. Measurements of runoff, soil temperature, snow depth, and frost depth were taken during the months of October through May during the years of 2003 through 2006. Data from the Singh et al. publication that were used in this study are listed in Table 1, along with observation methods.

Table 1. Data and observation methods for measurements from the Singh et al. (2009) study used for DHSVM calibration

Dataset	Measurement Frequency	Observation method
Soil temperature	15-min intervals	soil moisture probes
Frost depth	by event	frost tubes containing dye solution
Snow depth	by event	manual measurement
Runoff	by event	collection tanks at the base of hillslopes

3. Model

DHSVM (Andreadis et al., 2009; Storck et al., 1998; Wigmosta et al., 1994) is a physically based, distributed model developed for use in complex terrains that functions by solving water and energy balances. It can be applied over areas from plot scale to large watershed scale at sub-daily to daily timescales. The model includes a sufficient level of detail to represent important processes and feedbacks within the hydrology-vegetation system in a physically realistic manner. Models such as the Soil Water Assessment Tool (SWAT; Arnold and Fohrer, 2005) and the Water Erosion Prediction Project (WEPP; Laflen et al., 1991a,b) were also considered because of their ability to model crop development. Basic details on each model are given in Table 2. DHSVM was chosen because it has a higher degree of complexity than SWAT (Singh and Woolhiser, 2002), particularly in representing distributed soil and vegetation parameters, and because the WEPP watershed model cannot be applied to catchments as large as the combined North and South forks of the Palouse River.

Table 2. Models considered for use in this study and the advantages and limitations of each model.

Model	Advantages	Limitations
DHSVM	computationally intensive, high spatial variability of soil and vegetation parameters	no representation of dynamic crop growth
WEPP	fully models a wide variety of crop types and tillage practices	can only be applied to small watersheds, lower hydrologic complexity
SWAT	distributed model containing a crop growth component	lower level of complexity in hydrology calculations

DHSVM includes a two-layer canopy model for evapotranspiration and interception, an energy balance model for snow hydrologic processes and snowmelt runoff, a multiple layer unsaturated soil model, and a saturated subsurface flow model. Inputs required to run DHSVM include a digital elevation model (DEM) with a user-defined spatial resolution and GIS grid files representing vegetation, soil type, soil depth, and stream and road networks. Each grid cell can be assigned a unique value for vegetation and soil characteristics, and any number of classifications can be created to represent the properties of specific soil and vegetation types.

Wigmosta et al. (2009) performed a study in which the handling of winter infiltration and runoff by DHSVM was modified and coupled with the Hillslope Erosion Model (HEM; Lane et al. 1995a,b). Hydrology was computed by DHSVM, which produced a time series of surface runoff values to be used for erosion prediction by HEM. Wigmosta et al. (2009) added the Green-Ampt infiltration equation to DHSVM, which uses soil hydraulic conductivity as the basis for predicting infiltration. Their implementation of Green-Ampt incorporated a reduction of hydraulic conductivity during times when the soil was frozen according to the equation

$$\boldsymbol{K_{sef} = c_f K_{se}} \qquad (1)$$

in which K_{se} is the saturated hydraulic conductivity during normal conditions, K_{sef} is the saturated hydraulic conductivity for frozen soil and c_f is an adjustment factor. This method was originally used in the WEPP model. Wigmosta et al. (2009) reported that the model performed best when c_f was equal to 0.038, but other studies have reported that greater changes to conductivity must be applied to accurately model infiltration into frozen soil. Greer et al. (2006)

performed a study modeling winter infiltration with the WEPP model for the same PCFS plots used in this study and found that hydraulic conductivity needed to be reduced by a factor of 20,000 in order to accurately model winter field infiltration. Similarly, McCauley et al. (2002) reported that measured hydraulic conductivity in laboratory tests could be decreased by up to five orders of magnitude in frozen soils.

In this work, runoff and infiltration are handled in DHSVM through infiltration excess and saturation excess mechanisms (Doten et al., 2006). Infiltration excess is invoked when the soil is unsaturated, and saturation excess is used if the soil becomes saturated. The maximum infiltration rate is modified during soil freezing so that infiltration is decreased through the infiltration excess mechanism. An equation similar to that employed by Wigmosta et al. (2009) is used in which maximum infiltration rate is adjusted by

$$\boldsymbol{I_f = c_f I_u} \qquad (2)$$

in which I_f is the maximum infiltration rate for frozen soil, I_u is the maximum infiltration rate for unfrozen soil, and c_f is a factor of 0.005 when the soil is frozen. In reality the infiltration rate would approach zero as the soil became completely frozen and no water was able to move through the soil profile. Following Wigmosta et al. (2009), a soil temperature threshold of 0° C is used in DHSVM to determine when soil is frozen.

Three methods were tested for predicting when soil freezing occurs. The first method is the sensible heat flux model in DHSVM, which returns the surface temperature for each pixel through a surface energy balance using soil temperature observations for each modeled soil

layer. Measured soil temperatures from the PCFS site (Singh et al., 2009) at depths of 4, 16, and 32 cm were used, which are located approximately at the midpoints of the three soil layers modeled by DHSVM. The second method is a simple equation presented by Wigmosta et al. (2009) in which the near-surface soil temperature is used to predict whether soil is frozen or unfrozen by the equation

$$\boldsymbol{T_s^t = T_s^{t-1} + w(T_a^t - T_s^{t-1})} \qquad (3)$$

where T^t_s is the near-surface soil temperature at time t, T_a is air temperature and w is a weighting coefficient determined through calibration. The equation must be initialized with a measured or estimated soil temperature, and the model then relies solely on air temperature data for prediction. In this case T_s was estimated as being equal to air temperature during the first time step, and the model was given a spin-up period of two weeks. In using this method T_s is assumed to be zero if snow is on the ground because surface snowpack is generally warmer at the bottom, being close to 0 °C, and colder at the top, providing an insulating layer during very cold spells (Dingman, 2000). The third method is an even further simplified method in which the surface temperature is set equal to observed air temperature and soil is assumed to be frozen when the surface temperature is below 0° C. There is an expected source of bias in surface temperature prediction because each of the three methods predicts whether soil is frozen or unfrozen after the energy storage terms are no longer changing; none of the methods accounts for the warming and cooling of soil water or the amount of energy required for melting and freezing. Biases are therefore expected during freezing and melting periods.

Factors that affect the calculation of surface temperature in DHSVM include soil and vegetation albedo and transmittance of radiation through the overstory and understory (Wigmosta et al., 1994). The amount of radiation reflected from the surface will vary by the surface albedo and will differ between a light-colored crop residue and a darker bare soil. Novak et al. (2000) developed a model for simulating the distribution of radiation through surface residue that considers the effects of residue on shortwave and longwave radiation. In their work, multiple layers of stacked flat residue are considered; radiation through the residue is partially inhibited based on the percentage of ground covered and the number of residue layers. A transmissivity factor is applied to shortwave radiation, and longwave radiation is multiplied by a 'view factor' representing the percentage of soil visible from above residue. Novak et al. (2000) reported transmissivity values ranging from 0.03 to 0.76 based on the number of residue layers covering the surface. View factors for their model were calculated from transmissivity values; for a single residue layer, as would be the case in NT management, the view factor would be equal to the transmissivity. A similar transmissivity factor was added to the DHSVM calculations for radiation through the understory. Incoming shortwave radiation, R_s, is calculated in DHSVM using the equation

$$\boldsymbol{R_n = R_s T_u (1 - A_s)} \qquad (4)$$

where R_n is the net solar radiation reaching the surface, R_s is incoming solar radiation, T_u is the understory transmittance, and A_s is albedo. T_u was set to 0.76, which is the transmittance specified by Novak et al. (2000) for a single residue layer, and A_s was set to 0.25 for crop

residue and 0.1 for bare soil, as given by Breuer et al. (2003). A view factor representing the percent of soil visible through crop residue was added to the longwave radiation energy balance so that longwave radiation was calculated by

$$\boldsymbol{R_L = F_v \sigma T^4} \qquad (5)$$

in which R_L is longwave radiation, F_v is the view factor, σ is the Stefan-Boltzmann constant, and T is the temperature of the substance emitting radiation. F_v was set to 0.76 for crop residue, following Novak et al. (2000). This equation was applied as radiation passed through the residue layer, either being emitted upward from the soil surface or downward from the air or overstory vegetation.

4. Model input data

DHSVM was implemented over the North and South forks of the Palouse River at a 150 m grid cell resolution. Elevation input data were derived from the 1 arc second Shuttle Radar Topography Mission DEM (Farr, 1999). The DEM was processed into 150 m grid cells with ArcInfo (Esri, Inc.) and was utilized to delineate the study basin boundary and to create the soil depth and stream network data necessary for running DHSVM. Land cover was taken from the 30 m resolution 2001 NLCD dataset (Homer et al., 2001). Land cover classes are given in Table 3. Parameter values for each vegetation type were taken from literature, the NASA Land Data Assimilation Systems (LDAS) project (Mitchell, 2004), and model defaults. Parameter values and sources for each parameter are given in Table 4. The Soil Survey Geographic Database

(SSURGO; USDA-NRCS, 2005) developed by the Natural Resources Conservation Service (NRCS) was used as the source of soil data, and soil characteristic parameters were taken from literature and model defaults (see table 5).

Table 3. NLCD land cover types (Homer et al., 2001) in the combined North and South Fork Basins and South Fork Basin alone.

Landcover type	Percent cover in Upper Palouse Basin	Percent cover in South Fork Basin
1. Evergreen Forest	31.2	7.1
2. Urban	4.8	7.9
3. Shrub	8.7	2.4
4. Grassland	2.0	0.6
5/6. Agriculture (NT/ CT)	53.3	82.0

Table 4. Vegetation parameters used in DHSVM.

Vegetation parameters[a]	Evergreen Forest		Urban	Shrub	Grass	Ag (NT)	Ag (CT)
	1		2	3	4	5	6
	(overstory)	(understory)					
Impervious ground fraction [1,6]	0.0		0.5	0.0	0.0	0.0	0.0
Canopy overstory fractional coverage [2]	0.75						
Trunk space (fraction) [2]	0.5						
Aerodynamic extinction factor for wind through the overstory (fraction) [2]	3.5						
Radiation attenuation (fraction) [2]	0.5						
Maximum snow interception capacity (m SWE) [2]	0.04						
Ratio of mass release to meltwater drip from intercepted snow [2]	0.4						
Snow interception efficiency [2]	0.6						
Vegetation height (m) [3,5]	17.0	0.5	0.5	0.5	0.6	0.15	N/A
Maximum/minimum stomatal resistance [3,4]	6000/175	4500/125	4500/175	4500/175	4500/165	N/A	N/A
Light level where stomatal resistance equals two times the minimum stomatal resistance (fraction) [4]	0.108	0.108	0.108	0.108	0.108	N/A	N/A
Soil moisture threshold below which transpiration is restricted (fraction) [4]	0.33	0.13	0.13	0.13	0.13	N/A	N/A
Vapor pressure deficit above which transpiration is restricted (Pa) [4]	2500	3000	3000	3000	3000	N/A	N/A

[a] Sources for parameter are given in brackets - 1: model default; 2: North Fork Coeur d'Alene Watershed Assesment; 3: LDAS (Mitchell, 2004); 4: Whitaker et al. (2003); 5: Singh et al. (2009); 6: Greer et al. (2006); 7: NLCD (Homer, 2001)

Parameters used for NT and CT are listed in Table 4. Vegetation parameters for agricultural land were set differently for modeling CT versus NT. Parameters selected for CT represent cropland that is harvested in late summer and is subsequently tilled using conventional tillage methods during the fall, leaving the soil exposed through the winter months. Cropland under CT includes both fields that undergo a short fallow period between fall harvest and planting of spring wheat and those that are conventionally tilled after harvest and subsequently planted with winter wheat. NT parameters represent land that is not tilled after harvest, in which either spring wheat or winter wheat is planted directly into soil covered with residue from the previous crop. Vegetation was modeled as bare ground for CT and as an understory for NT. Since the residue layer consists of dead vegetation during the non-growing season, the model represented this component as dead plant mass during the appropriate months, which allowed interception and evaporation from the understory to continue while eliminating transpiration processes during the non-growing season. However, the crop understory under NT conditions during the growing season was modeled using corresponding NT vegetation parameters so that summer hydrologic calculations would include transpiration from the growing crops.

Table 5. Soil parameters used in DHSVM.

Silty loam soil	
Soil Parameter[a]	Value
Lateral conductivity (m/s) [1]	5.92E-04
Exponential decrease in conductivity [7]	3.0
Maximum infiltration rate (m/s) [1]	3.00E-06
Number of soil layers [7]	3
Porosity (fraction) [3]	0.50
Pore size distribution index [4]	0.26
Bubbling pressure (m) [4]	0.21
Field capacity (fraction) [5]	0.34
Wilting point (fraction) [5]	0.14
Bulk density (kg/m^3) [5]	1330
Vertical conductivity (m/s) [5]	2.96E-06
Thermal conductivity ($W/m \cdot K$) [6]	7.01
Thermal capacity ($J/m^3 \cdot K$) [6]	1.40E+06

[a] Sources for parameter are given in brackets - 1: calibration parameter; 2: Greer et al. (2006); 3: Alberts et al. (1995); 4: Maidmont (1993); 5: SWC model (Saxton, 1986); 6: Ochsner, 2001; 7: Model default

For observed meteorological data, we applied the University of Washington 1/16th degree 1915 – 2006 precipitation and air temperature grids (Elsner et al., 2009) to provide consistent spatial and temporal model inputs. The 1915-2006 historical data are gridded observations from the National Climatic Data Center Cooperative Observer (Co-Op) network with adjustments to account for orography using PRISM data (Daly et al. 1994) and a changing station network in time (Hamlet and Lettenmaier 2005). The data were disaggregated to 3-hour intervals using a method described by Cuo et al. (2009). As DHSVM requires hourly meteorological data to run simulations, daily data were run through a preprocessor following Thornton and Running (1999) to estimate solar radiation from daily temperature extremes. Additionally, soil temperature observations that were necessary to run model calculations of the sensible heat flux were taken from the University of Idaho Moscow Co-op station made

available through the National Climatic Data Center (NCDC, 2009). Daily maximum and minimum 10 cm soil temperatures were converted to three-hour temperatures and were filtered with a Kolmogorov-Zurbenko filter as given by Wise et al. (2005) to create soil temperature data for three soil layers. Filtering was necessary because the lower soil layers are insulated by the upper layers, dampening the daily fluctuations in temperature. The filter is a simple low pass filter with the equation

$$\boldsymbol{Y_i = \frac{1}{m}\sum_{j=-k}^{k} A_{i+j}} \qquad (6)$$

where k is the number of values on either side of the targeted value, i is the current time step, and j ranges from $-k$ to k for the summation; m is equal to $2k$ +1, and A is the input time series. A value of k = 3 was used, and the filter was run three times. The resulting temperatures were gridded to the same 1/16th degree grid as the climate forcing by scaling soil temperature by the ratio of observed air temperatures at the Moscow Co-op station to air temperature at each grid point, according to the equation

$$\boldsymbol{\frac{T_{s\,(Co-op)}}{T_{a(Co-op)}} = \frac{T_{s(grid)}}{T_{a(grid)}}} \qquad (7)$$

where $T_{s(grid)}$ is the soil temperature at each climate forcing location calculated using soil temperature, T_s, at the Co-op station and air temperature, T_a, from the Co-op station and gridded climate data.

5. Basin scale model calibration

Calibration for the entire basin was performed using streamflow records from USGS stations located at Colfax immediately downstream of where the North and South Forks meet, and at Potlatch on the North Fork of the Palouse River (see Figure 1 for gauge locations). Data records are available from Oct. 1963 through Sept. 1995 for the Colfax station, and from Nov. 1966 to present for the North Fork Palouse River at Potlatch. The calibration period was Oct. 1984 through Sept. 1990, and the validation period was Oct. 1990 through Sept. 1995. The lengths of the calibration and validation periods were limited because soil temperature data are only available from Jan. 1982 until present for running the DHSVM sensible heat flux model. A two year spin-up period was used before the beginning of the calibration run, and the states of model fluxes from the end of the calibration period were used to start the validation run. All soil and vegetation parameter values were set to realistic numbers according to literature (see Tables 4 and 5), and lateral hydraulic conductivity was used as the single calibration factor. Model performance was evaluated using the Nash-Sutcliffe efficiency statistic (Nash and Sutcliffe, 1970), calculated by

$$\boldsymbol{N.S.} = \mathbf{1} - \frac{\sum_{i=1}^{N}(Q_{obs}^{i} - Q_{sim}^{i})^{2}}{\sum_{i=1}^{N}(Q_{obs}^{i} - \bar{Q}_{obs})^{2}} \qquad (8)$$

where Q^{i}_{obs} is observed streamflow at time step i, Q^{i}_{sim} is modeled streamflow, and N is the total number of time steps in the evaluation period. USGS streamflow observation records during the calibration and validation periods were available for the North Fork at Potlatch and

the combined North and South Forks at the basin outlet near Colfax. Observation periods available for each station are shown in Table 6.

Table 6. Stream gauge stations used in evaluating model performance.

Gauge location	River section	Available streamflow records
Potlatch	North Fork	Nov 1966 - present
Colfax	Palouse River (downstream of where N. and S. forks intersect)	Oct 1975 - Sept 1995

6. Field scale model calibration

In order to investigate the effects of tillage on soil water storage, DHSVM was first run at the field scale over the two experimental plots from the Singh et al. (2009) study that were maintained separately under CT and NT conditions. Model calibration at this scale was done by adjusting the maximum infiltration rate so that infiltration will decrease during periods when the ground is frozen. To investigate surface temperature differences between management types, CT was assigned an albedo value of 0.1 and NT was assigned a value of 0.25 (Breuer et al., 2003). For calibration at this scale, DHVSM was run for the period of October 2003 through September 2007 for a single 150 m pixel overlaying the field plot. Field runoff was calibrated based on the percent change in the fraction of precipitation that became runoff during frozen and unfrozen conditions. For field calibration, the model was not calibrated for summer hydrology because the focus of this work is on the winter period prior to crop growth.

7. Management scenarios

The calibrated model was applied to investigate two scenarios in the South Fork basin: one in which all agricultural area was modeled with CT parameters, and one in which agriculture was modeled with NT parameters. The model was run for the 2004-2005 winter season from November to April in order to determine differences in water capture and storage between NT and CT.

Two equations were used to estimate crop yield based on spring water content and precipitation received during the growing season. The first is an equation presented by Leggett (1959) for predicting crop yields in annually farmed regions of the Palouse:

$$\boldsymbol{Y = 146(SM + GR) - 1480} \qquad (9)$$

where Y is crop yield (kg/ha), SM is soil moisture (cm) on April 1st, and GR is rainfall (cm) received between April 1st and harvest. In this equation, at least 10 cm of water are required for producing a wheat crop, and each additional cm of water results in a 146 kg/ha yield increase. Results from this equation were compared to a similar equation given by Schillinger et al. (2008), which is a generalized equation for both annually cropped areas and regions that employ a fallow season in the Palouse:

$$\boldsymbol{Y = 150(SM) + 174(SR) - 986} \qquad (10)$$

where SR is the amount of spring rainfall received during April, May, and June. Water content on April 1st was taken from DHSVM output, and spring and growing season precipitation were taken from the Pullman NCDC station, assuming that crops were harvested on the 15th of August for determining GR. Both equations imply a linear relationship between available water and crop yield and do not account for the fact that there is a point when additional water will not increase yield due to other limiting factors. The equations are beneficial for simple yield estimation, but are not meant to replace a fully coupled hydrology and cropping systems model.

RESULTS AND DISCUSSION

1. Basin scale calibration

The N.S. model efficiency during the calibration period was 0.69 for the Palouse River at Colfax and 0.54 for the North Fork Palouse River at Potlatch. The level of accuracy at Colfax, which is the basin outlet, and the Potlatch station compares well with DHSVM performance from previous studies, which have reported efficiencies in the range of 0.57 to 0.91 (Beckers and Alila, 2004; Thyers et al., 2004; Wigmosta and Burges., 1997). The model produced the most accurate results when lateral saturated hydraulic conductivity, the single calibration parameter, was set to 5.92E-4 m/s. For comparison, the value of vertical conductivity of the silt loam soil was set to 2.96E-6 m/s as given by Chow (1988). Error statistics for the calibration and validation periods are given in Table 7.

Table 7. Nash-Sutcliffe model efficiency, RMSE, and relative bias at three gauge stations during the periods of calibration and validation.

	N. S.	RMSE (m^3/s)	R. Bias (%)	N. S.	RMSE (m^3/s)	R. Bias (%)
		Calibration			Validation	
Station		(Oct 1984 - Sept 1900)			(Oct 1990 - Sept 1995)	
Potlatch	0.54	7.3	-55.4%	0.60	6.8	-16.3%
Colfax	0.69	8.2	-26.4%	0.64	8.6	38.4%

Modeled and predicted streamflow at Colfax during the calibration period are shown in Figure 2. The calculated RMSE during this period was 8.2 m^3/s, which is slightly larger than the mean observed flow of 8.0 m^3/s. The relative bias for streamflow at Colfax was -26.4%,

indicating that the total amount of streamflow was under-predicted by the model. During the first four years of calibration, DHSVM seemed to predict peak flows reasonably, but in the last two years of calibration one large flow event was over-predicted and three peak flows were under-predicted, being approximately half of the observed flow at the Colfax gauge. Incorrect predictions of peak flows could have been caused by scarcity of data from NCDC stations, particularly in the eastern portion of the upper Palouse Basin. Because this area receives a higher amount of precipitation than the rest of the Palouse, any error in precipitation measurement would translate to significant error in streamflow prediction. Base flows were generally over-predicted by a small amount, with the average predicted base flow being 0.8 m^3/s higher than observed base flow during the summer months.

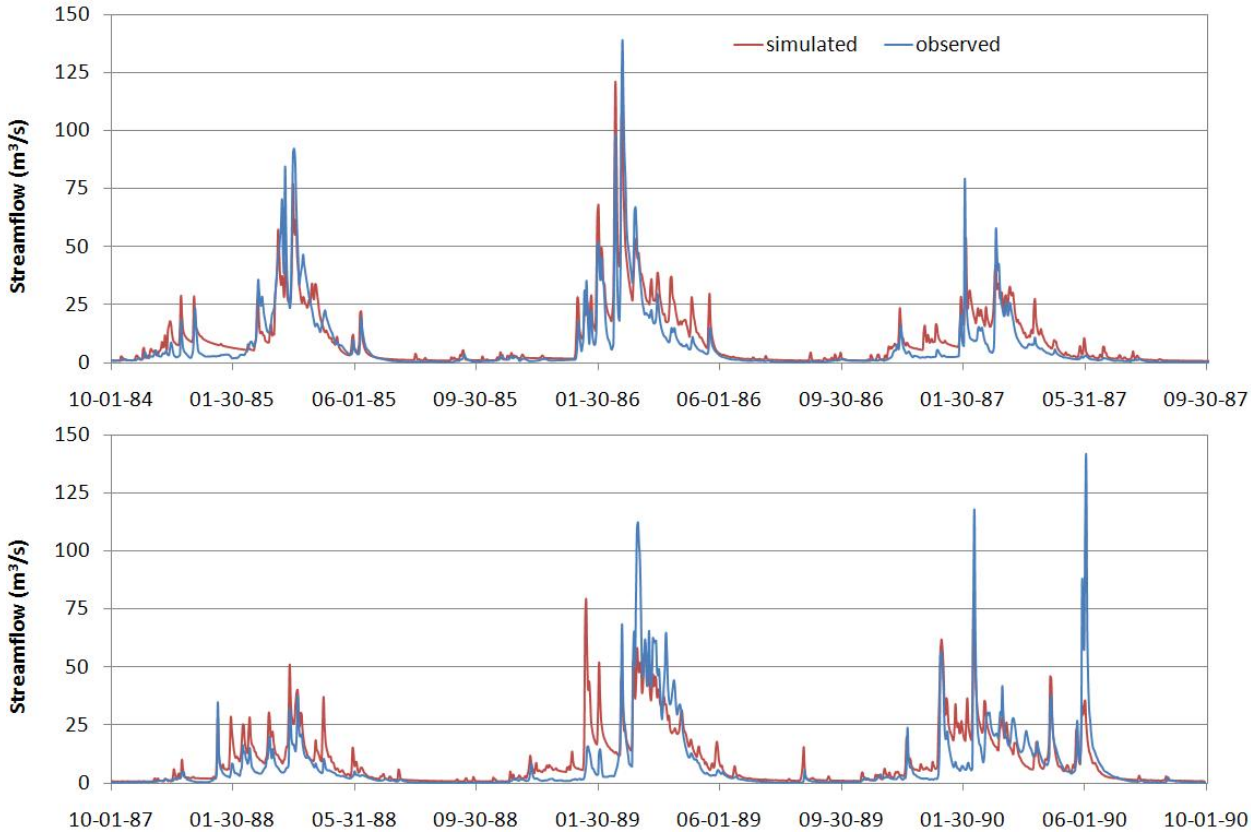

Figure 2. Observed and predicted streamflow for the Colfax stream gauge during the calibration period.

Figure 3 illustrates the average monthly streamflows for Colfax during the calibration period. DHSVM had a tendency to over-predict flow during the months of November through February, but observed and predicted monthly flows were similar for the months of March through June. Over-prediction in the rising limb of the annual hydrograph may be a result of sparse temperature records from NCDC stations; because the overall volume error is small, inaccurate temperature data could cause error in the timing of snowmelt-dominated winter and spring runoff. Total predicted flow during the peak month of March was 856 m^3/s, as compared to a total observed flow of 921 m^3/s.

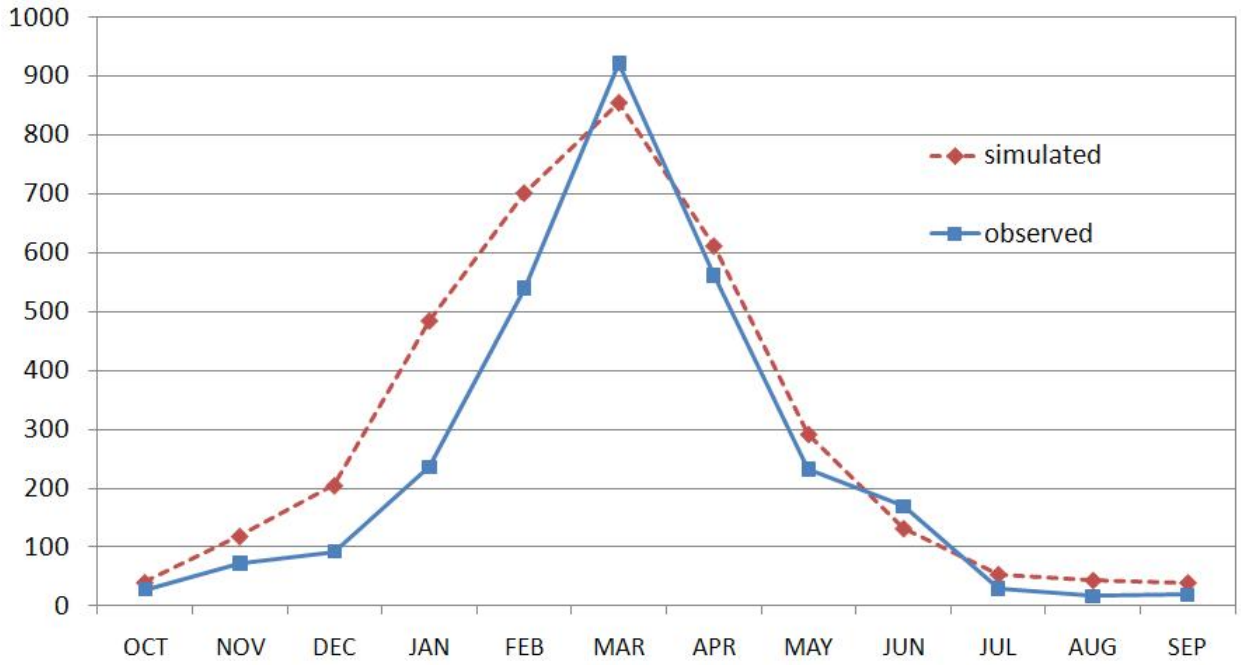

Figure 3. Monthly biases during calibration at Colfax.

Model results and observed streamflow for the Potlatch stream gauge during the calibration period are shown in Figure 4. The calculated RMSE for streamflow at this gauge was 7.3 m^3/s, compared to an average flow of 5.5 m^3/s, and the relative bias was -55.4%, indicating that, similar to the Colfax simulations, total streamflow was under-predicted at Potlatch. Modeled peak flows were well below observed peak flows at Potlatch, with streamflow predicted by DHSVM being less than half of the peak gauge flow during all years except for the winter of 1987-1988 when streamflow was much lower in comparison to other years. Low peak flows can also be seen in Figure 5, which illustrates the average monthly flows at the Potlatch gauge. Predicted flows biased toward the low side during February, March, and April, with the average modeled flow in March being approximately half of observed flow. As with the Colfax station, differences in observed and predicted streamflow may be caused by variation in

precipitation and other climate variables throughout the basin not captured in the meteorological forcing data due to a lack of thorough coverage of NCDC stations in the region, particularly in the upper section of the North Fork (see Figure 1 for station locations).

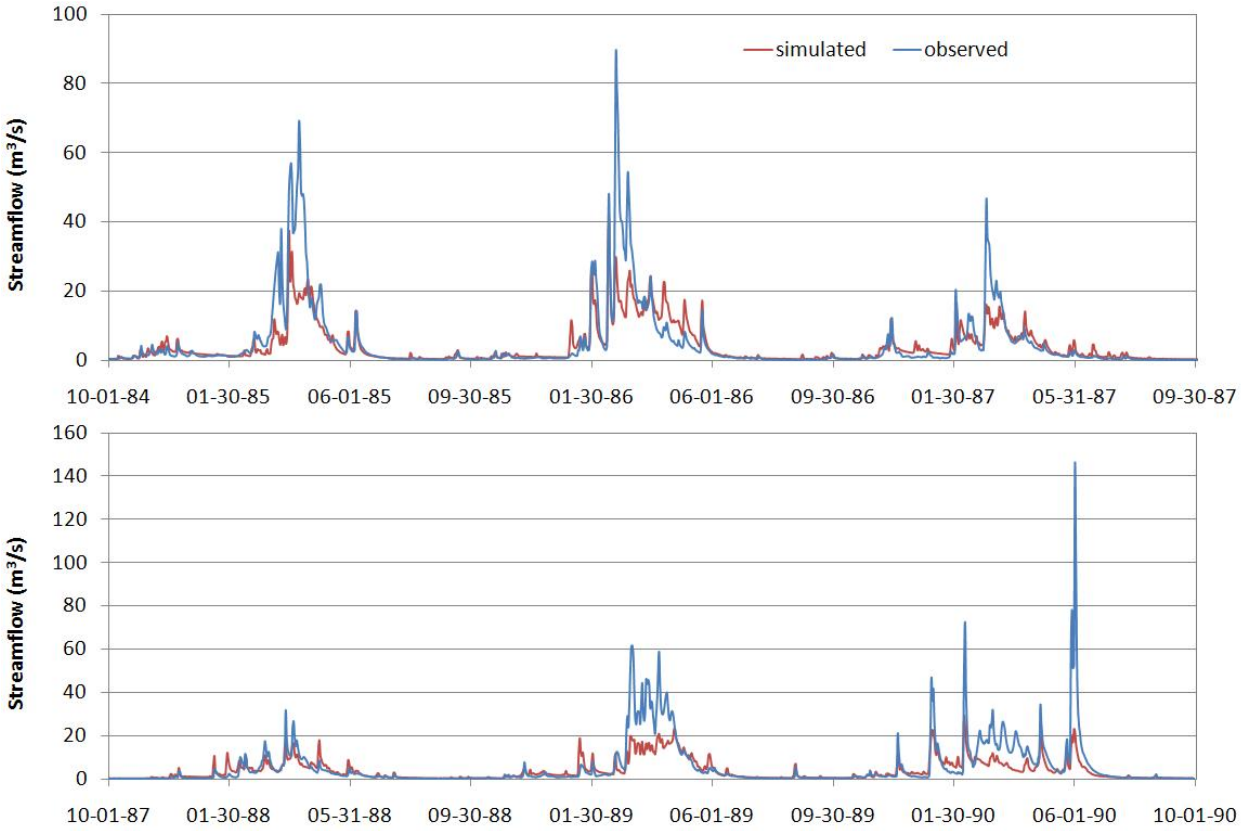

Figure 4. Observed and predicted streamflow for the Potlatch stream gauge during the calibration period.

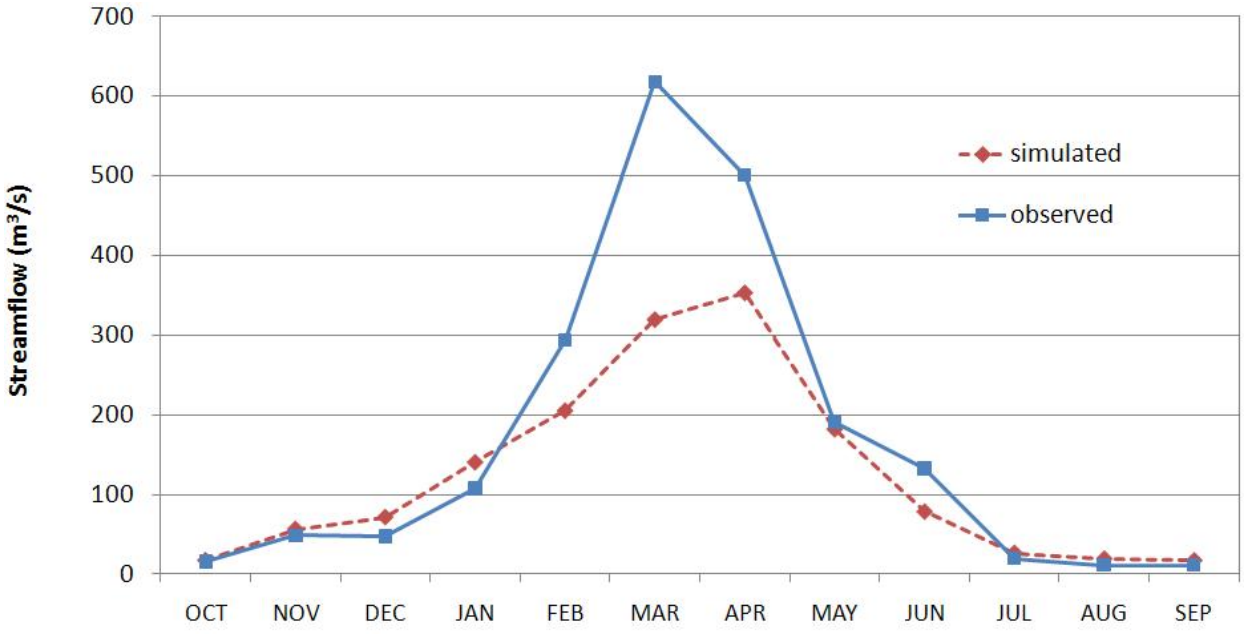

Figure 5. Monthly biases for Potlatch during calibration.

During the validation period, model error statistics were similar to those calculated for the calibration period. N.S. model efficiency was 0.60 at Potlatch, and RMSE was 6.8 m^3/s, indicating a better performance both efficiency and RMSE. Prediction at Colfax yielded a N.S. efficiency of 0.64 and a RMSE of 8.6 m^3/s. Observed and modeled streamflow during the validation period are depicted in Figure 6, and model error statistics are listed in Table 7. As in the calibration period, underestimation of peak flow events occurred at both Colfax and Potlatch during the five year validation period. The difference between observed and predicted flows tended to be greater at Potlatch, with the greatest amount of under-prediction seen in the third and fifth years of validation.

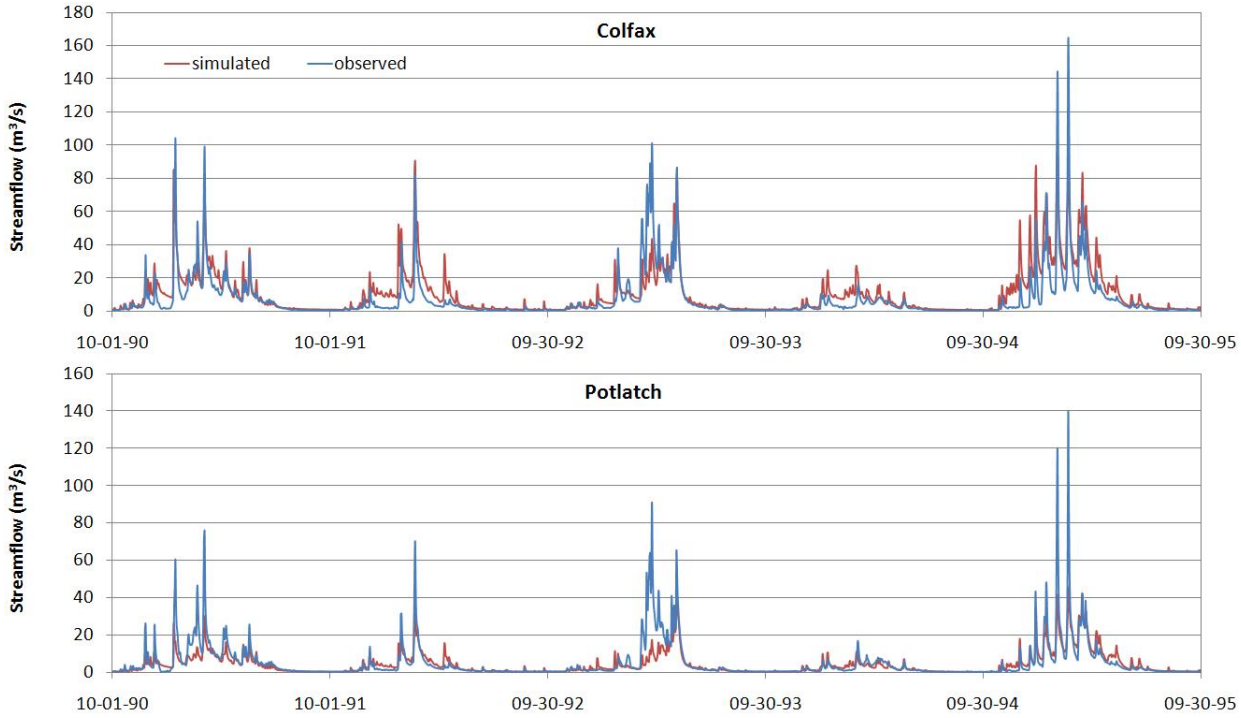

Figure 6. Observed and modeled streamflows at Colfax and Potlatch during the validation period.

2. Field scale calibration

Field scale calibration was performed by using the maximum infiltration rate as the calibration parameter. During calibration, the objective was to produce the same number of runoff events as observed at the PCFS site and to increase runoff during periods with frozen soil by the same amount that observed runoff was increased. Runoff observed by Singh et al. (2009) is shown in Figure 7. During all four winter seasons, runoff events were prevalent on the CT plot while the NT plot experienced only three events, each with a runoff volume of less than 1 mm.

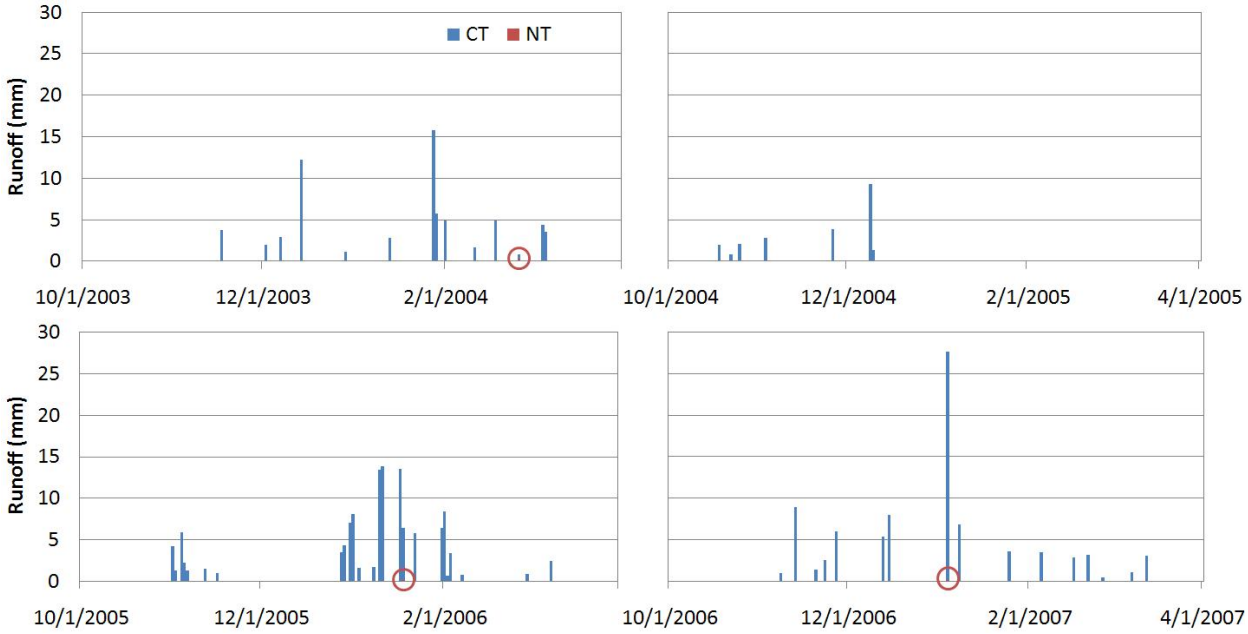

Figure 7. Observed runoff recorded by Singh et al. (2009) from CT and NT plots at the PCFS site for the winter seasons of 2003 through 2007. The three runoff events of less than 1 mm that occurred on the NT plot are circled in red.

DHSVM was initially run at the field scale with the same calibrated input parameters used in the basin scale calibration (see Tables 4 and 5) to attempt to simulate these observed runoff events. No runoff was predicted when running the model with either CT or NT vegetation parameters for the single pixel overlying the PCFS site. Because of this, the maximum infiltration rate parameter was decreased from 3.0E-06 to 2.0E-07 m/s for field scale model runs. By using this infiltration rate, the number of simulated runoff events was closer to the number of observed events, although the volume of runoff was larger for simulated runoff events. The need for a different maximum infiltration rate in field-scale versus basin-scale calibration may be caused by preferential sub-surface flow pathways. At times when runoff is produced on individual hillslopes at the PCFS site there may not necessarily be runoff on a

larger scale if surface water later infiltrates the soil and a greater amount of water movement occurs below the surface.

The effect of frozen soil on runoff events at the PCFS was examined by comparing the total amount of available water during a precipitation or snow melt period to the amount of runoff collected during the same period. The ratio of observed runoff to available water for each event during the study period is shown in Figure 8. Available water was calculated as the as the sum of rainfall measured at the Pullman 2-NW NCDC station and the change in snow water equivalent (SWE) determined from observed snow pack depth measured by Singh et al. (2009). SWE was calculated according to the method suggested by the Natural Resources Conservation Service (NRCS, 2010), assuming a snow to liquid water density ratio of 0.05 at -10° C and 0.20 at 0° C, with the ratio being linearly interpolated between 0.05 and 0.20 at temperatures between -10° and 0° C. Along with SWE, precipitation from the day of runoff collection plus the two previous days was used in calculating available water. The previous days were considered because measurements were typically taken from the runoff collection tanks on the day after a storm event meaning that the water level measured was a representation of total runoff for at least a two day period and possibly longer depending on what time of day runoff occurred and measurements were taken. In some cases the measured runoff was greater than the calculated available water. This is likely because precipitation measurements at the Pullman station did not accurately represent the precipitation received at the PCFS site. If observed runoff was greater than calculated available water, it was assumed that 100% of available water contributed to runoff.

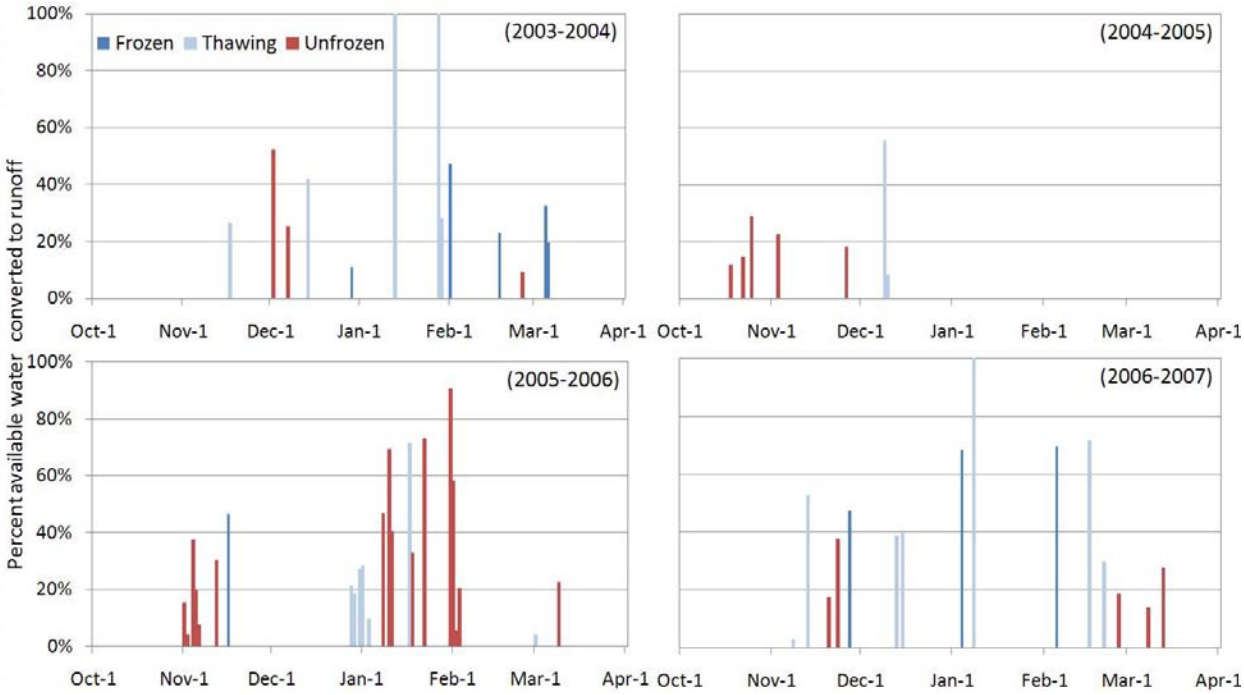

Figure 8. Percent of available water from change in observed SWE and precipitation contributing to runoff on the CT field plot for frozen, thawing and unfrozen runoff events during the winters of 2003-2004 through 2006-2007.

The largest runoff events occurred on the CT plot during frozen and thawing conditions. Frozen conditions were determined by frost tube measurements and soil temperature readings at a depth of 2 cm as reported by Singh et al. (2009), and the soil was considered to be thawing when frost tubes indicated that the frost layer had retreated either from the surface or the bottom of the frost layer since the previous measurement. During 74 different runoff events on the CT plot, 47% and 44% of available precipitation and snowpack became runoff during frozen and thawing soil conditions, respectively; only 30% of available water contributed to runoff during unfrozen soil days. Results are summarized in Table 8. The three runoff events on the NT plot (not pictured) occurred on unfrozen ground with no snowpack; in all events less than 5% of precipitation became runoff.

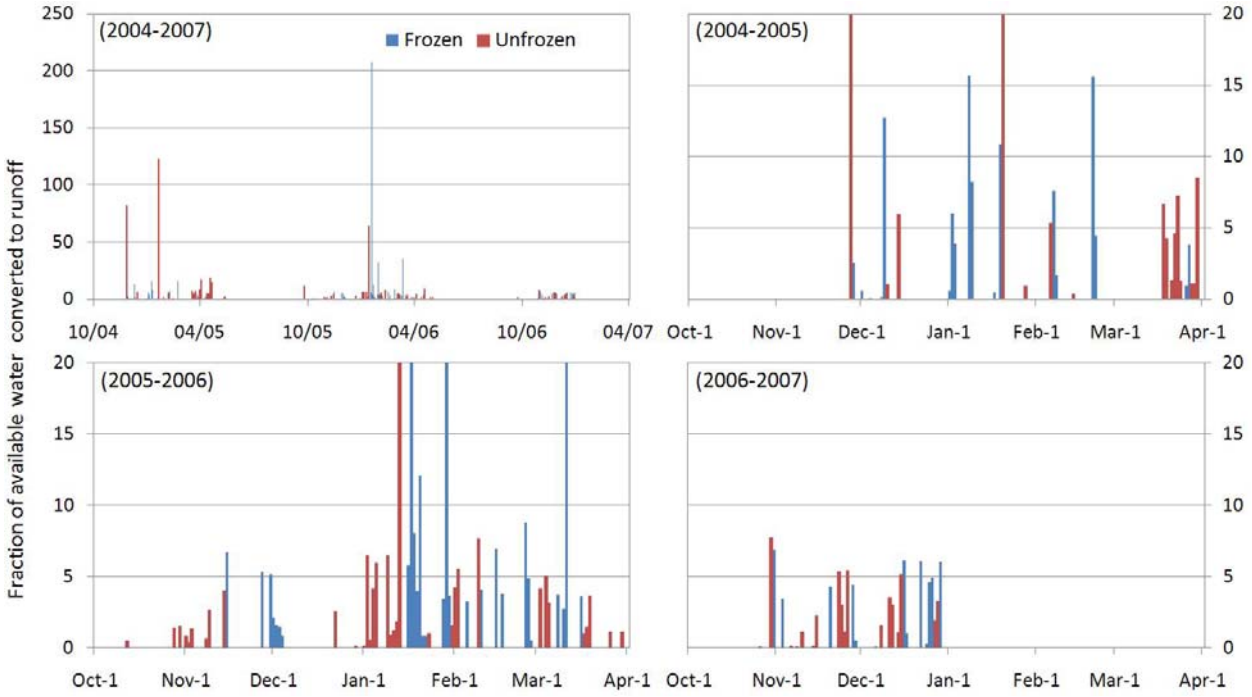

Figure 9. Percent of available water from precipitation and DHSVM modeled change in SWE contributing to runoff on a single pixel overlaying the PCFS site. The upper left panel illustrates the entire period and the remaining three panels depict each individual season at a different scale so that individual events can be seen more clearly.

DHSVM predictions for the fraction of available water converted to runoff are shown in Figure 9. In this case, conditions were considered to be frozen if modeled soil temperature was less than 0° C during at least half of the day, or 4 out of 8 time steps. In many events, the predicted runoff was greater than the amount of available water. This was a result of runoff contribution from multiple DHSVM grid cells; although the model output used in field calibration was from a single pixel, runoff is calculated in DHSVM as the sum of runoff produced on that pixel plus runoff routed to that pixel from grid cells located at higher elevations.

Table 8. Percent of observed and modeled precipitation and change in snow water equivalent contributing to observed runoff on the CT plot for all runoff events during the winters of 2003-2004 through 2006-2007.

	Observed				Modeled	
	Number of events	Average 3-day precip plus ΔSWE	Average Runoff	Percent available water contributing	Number of events	Percent available water contributing
Frozen	10	13.4 mm	5.9 mm	48%	55	506%
Thawing	22	16.6 mm	5.9 mm	44%		
Unfrozen	42	12.9 mm	3.4 mm	30%	43	252%

By reducing the maximum infiltration rate by a factor of c_f = 0.05 when the ground was frozen it was possible to reduce infiltration so that modeled storm events produced a higher amount of runoff. This reduction in infiltration rate is not as large as the reduction by a factor of 20,000 reported by Greer et al. (2006), but is a larger reduction than the c_f factor of 0.038 used by Wigmosta et al. (2009). For 41 modeled runoff events the amount of runoff was increased from 252% of available water to 506% because of soil freezing. While these fractions of runoff to available water are not close to the observed fractions of 48% for frozen soil and 30% for unfrozen soil, the percent increases are similar between observed and modeled events. During freezing, the increase in observed runoff by a factor of 1.60 from 30% to 48% available water is similar to the modeled increase by a factor of 2.01 from 252% to 506%.

Results from field scale calibrations are shown in Figure 10. The timing of modeled runoff generally matches up with observed runoff with some exceptions during the first winter season when several large events were predicted but not observed and during the third season when several events occurred that were not predicted. The volume of runoff is generally predicted to be higher than observed runoff. This is expected because DHSVM calibrations were

based primarily on the number of runoff events predicted and the difference between runoff on frozen versus unfrozen ground.

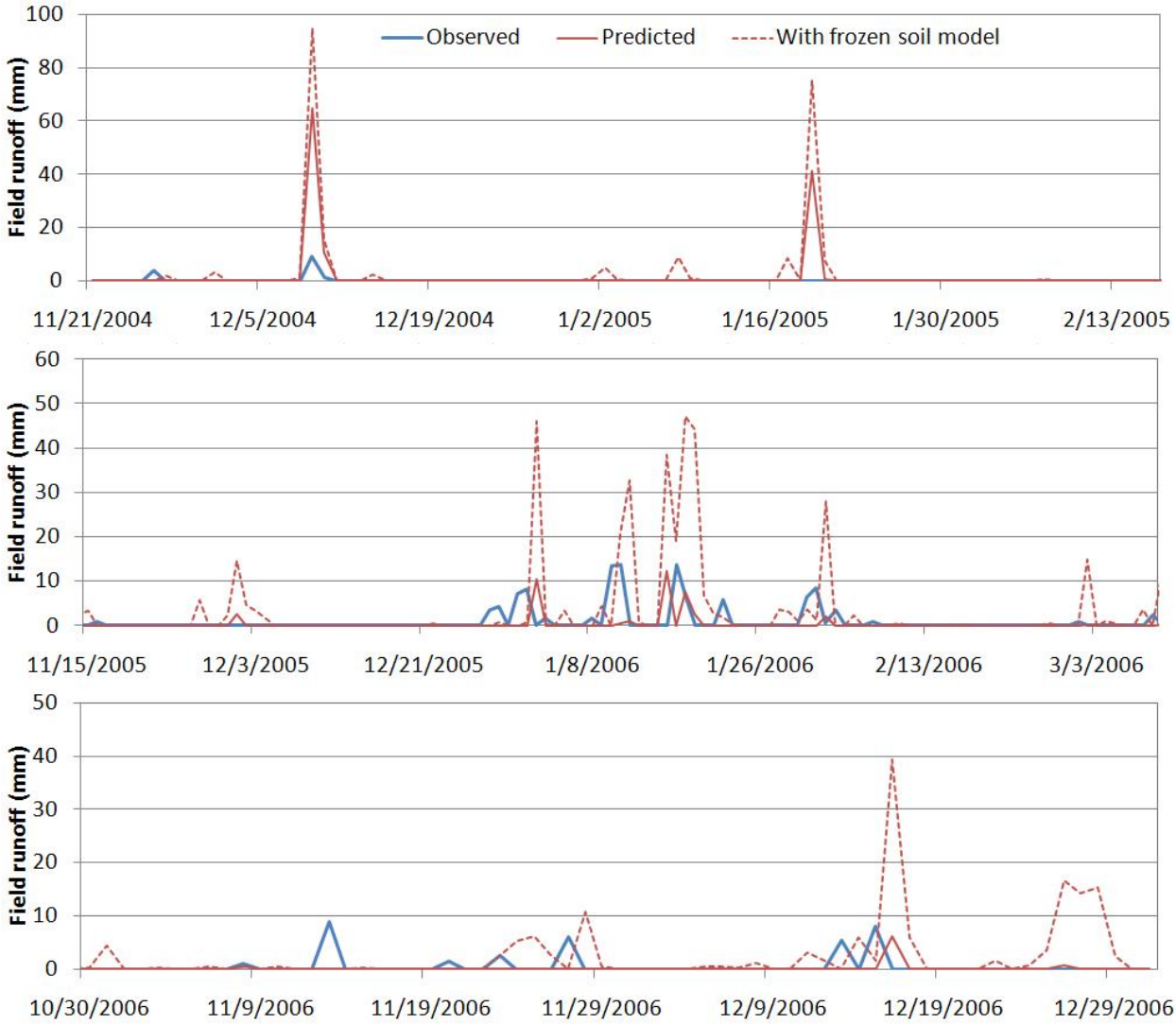

Figure 10. Predicted runoff with and without the effects of frozen soil for a single pixel overlaying the PCFS site during three winter seasons. Periods between the first and last frosts of each year are shown.

Calibration at the field scale was done using runoff data from the CT plots. Calibration was not possible on the NT plot because there were not enough runoff events to determine the change in runoff volume during freezing. The absence of any runoff events on the NT plot may

be caused in part by the effect of the insulating crop layer preventing the ground from freezing, but is also likely affected by increased retention of surface water by crop residue. It is possible that freezes occurred on the NT plot, but that melting snow and precipitation were captured and stored in the residue until temperatures increased enough to melt the frost layer and allow infiltration again.

3. Prediction of freeze and thaw events

Predicted and observed surface temperatures for the winter seasons of 2004-2005 through 2006-2007 are shown in Figure 11. The N.S. model efficiencies for the three methods of estimating surface temperature are shown in Table 9 (see Methods section for a description of each method). Model performance was evaluated using 3-hour model predictions and observed surface temperatures at a depth of 2 cm from the PCFS site (Singh et al., 2009) for the winter seasons of 2004-2005 through 2006-2007. Model efficiency for predicting surface temperature was 0.60 when using method 1. Methods 2 and 3 had efficiencies of 0.66 and 0.67 respectively, with a value of w = 0.9 used in method 2. Method 2 gave better predictions as the weighting coefficient w was increased and approached a value of 1.0. With a value of 1.0 for w, the equation considers only air temperature and ignores the surface temperature calculated for the previous time step and, therefore, is identical to method 3. This may be an indication that surface temperature on the PCFS site is primarily a function of air temperature at the time of observation and that air temperature from the previous time step does not greatly affect surface temperature.

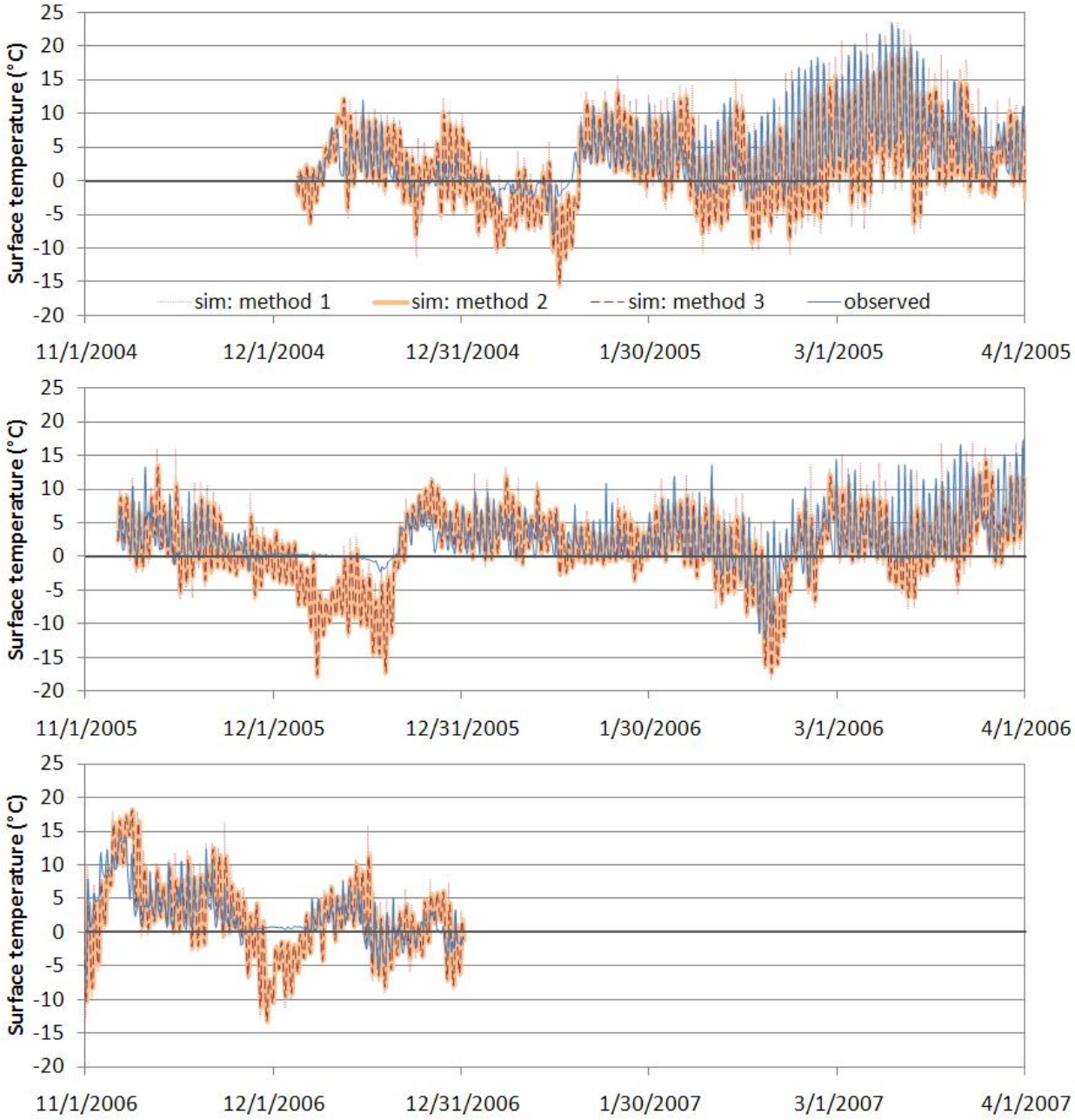

Figure 11. Predicted surface temperature for the three methods and observed soil temperature at a depth of 2 cm as measured by Singh et al. (2009).

There is at least one period during each year in which surface temperature observations appear to be close to 0° C while the three prediction methods indicate below-freezing soil temperatures. This occurred most prominently during early December of 2005 and 2006. The

under-predicted temperatures are likely due to the simplified prediction methods that do not include heat storage effects such as the transfer of energy when soil water temperature changes or the latent heat that is released or received during freezing or melting. A significant energy loss is required to cool and freeze water; if this energy loss was not considered in calculating surface temperature it would be expected that temperature would be underpredicted by a considerable amount as can be seen in Figure 11. Methods 2 and 3 may be further biased because they utilize only air temperature and do not consider the insulating effect of snow pack cover.

The model also has difficulty in predicting surface temperature during the spring months; soil temperatures are over-estimated beginning in late February or March and persisting through April. This may also be a result of the model missing some heat storage effects as mentioned above, causing excess heat to be kept in the soil, or could be caused by error in lapsed air temperatures from the Pullman PCFS station that do not correctly represent temperatures at the PCFS site.

Table 9. Comparison of model efficiency in predicting surface temperature for methods 1, 2, and 3.

Method	N. S. efficiency
1: DHSVM sensible heat flux	0.60
2: Wigmosta equation (w = 0.9)	0.66
3: Air temperature	0.67

Although method 1 had the lowest model efficiency during the evaluation period, it was chosen for use in further model runs because it allows the surface energy balance in DHSVM to interact with incoming radiation that is affected by the albedo and transmissivity of the soil and

vegetation. This allows the residue layer to have an effect on the surface soil temperature so that frozen ground can be modeled under different tillage conditions.

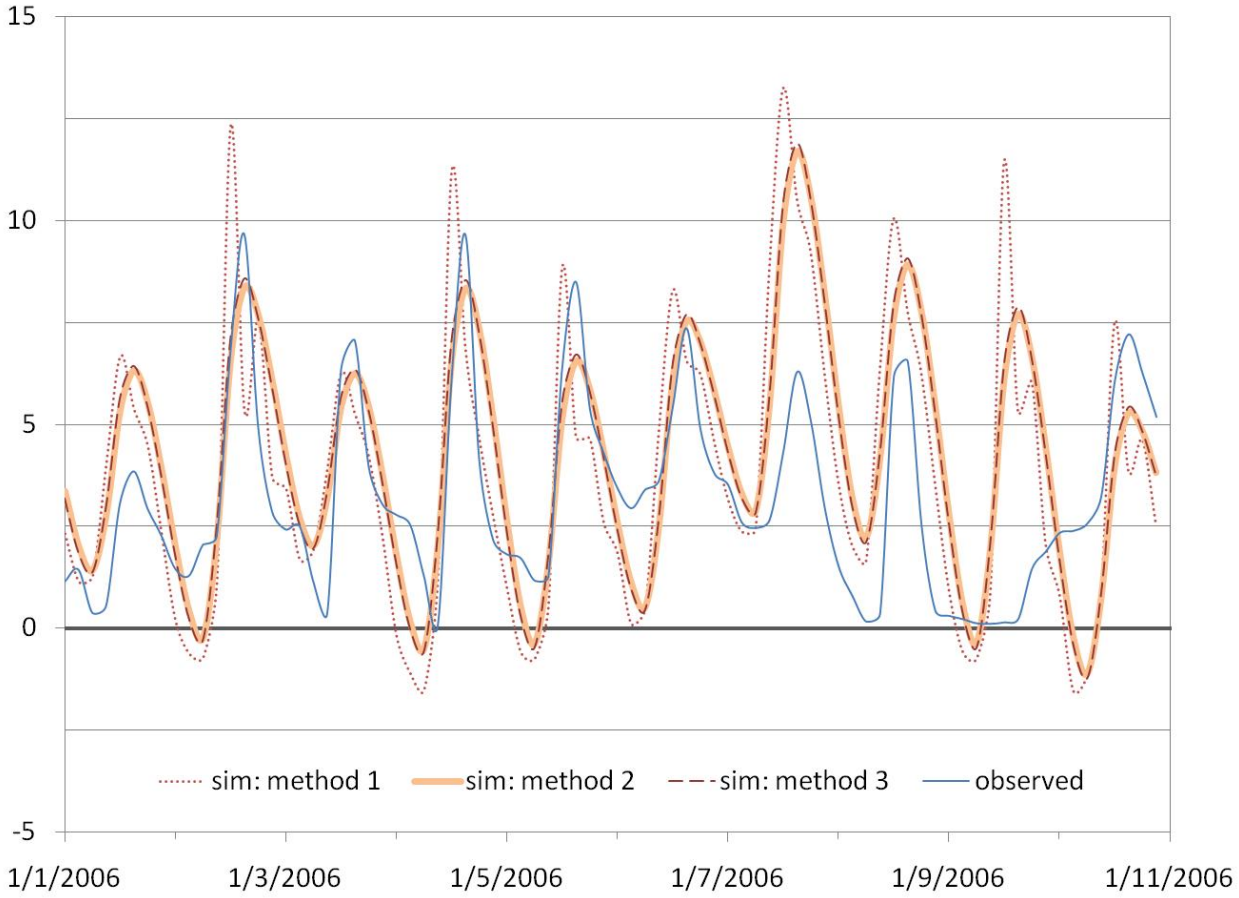

Figure 12. Observed 2 cm soil temperature (Singh et al., 2009) on the CT plot compared to surface temperature predicted by method 1: the DHSVM sensible heat flux algorithm, method 2: equation used by Wigmosta et al. (2009), and method 3: air temperature from model forcing data.

Figure 12 illustrates the difference between observed surface temperatures and the three prediction methods on the CT plot for the period of January 1 through January 11, 2006. This time frame represents a sample from the three winter seasons used in analysis. Four separate runoff events occurred during this period when the temperature was close to the freezing point, making the prediction of surface temperature essential for accurately modeling infiltration and runoff under the correct soil state. The three prediction methods agree with

each other in indicating that the soil is frozen at five separate times during the 10-day period. Observed temperature during this time period never drops below zero, although temperatures below 0.5° C are observed during two of the predicted freezes. Frost tube measurements indicate that the ground was in a thawing state during January 1 through 3, which coincides with one of the predicted freezes. Differences in modeled and observed temperatures are likely caused by the use of gridded climate data that are interpolated to a $1/16^{th}$ degree grid from NCDC station observations. The NCDC station that is nearest to the PCFS site is located in Pullman, approximately 1.6 kilometers from the research site, as can be seen in Figure 1. Differences in terrain and elevation, as well as the fact that the PCFS is located in a rural setting and the NCDC station is in located in town may contribute to differences in temperature, such as are seen in Figure 12.

The model predicted the state of the soil, whether frozen or unfrozen with an accuracy of 81% on the PCFS study area during the winter seasons of 2004-2005 through 2006-2007. For assessing frozen soil predictions, the winter season was defined as the time period from the first to last observed frosts of each winter season, except during the last season when the meteorological dataset used for prediction ended on January 1, 2007. DHSVM correctly predicted 89 out of 115 observed frozen soil days on the CT plot during the three winter seasons and 126 out of 145 unfrozen days (see Table 10). On the NT plot 74 out of 104 frozen days were accurately predicted, and 142 out of 162 unfrozen days were predicted. The model tended to miss predictions of frozen days more often than unfrozen, which caused a fewer number of times that increased runoff on top of frozen soil was modeled. While the surface temperatures calculated by DHSVM are generally realistic based on the 0.62 N.S. model

efficiency calculated above, there is a certain amount of error that makes the determination of frozen soil difficult because a single degree difference in surface temperature prediction can make the difference between freezing and thawing soil. The ability to predict soil state correctly for 81% of the winter season is slightly lower than results reported by Wigmosta et al. (2009), who found that soil state could be predicted correctly 87% of the time, but is reasonable considering that on-site air temperature observations were not used.

Table 10. Model performance in predicting historical freeze events on the PCFS site. Total numbers of frozen and unfrozen events are given for each season along with the number of those events correctly predicted by DHSVM.

	2004-2005		2005-2006		Winter 2006	
	Days	Correct Pred.	Days	Correct Pred.	Days	Correct Pred.
Frozen (CT)	34	29 (85%)	49	37 (76%)	32	23 (72%)
Unfrozen (CT)	48	40 (83%)	66	58 (88%)	31	28 (90%)
Frozen (NT)	37	28 (76%)	39	26 (67%)	28	20 (71%)
Unfrozen (NT)	51	43 (84%)	76	66 (87%)	35	33 (94%)
Average		82%		80%		82%

Observations from the PCFS indicate that NT generally had a higher temperature than CT in the upper section of the soil profile although the difference was relatively small, being on average less than 1.0° C for all years. Singh et al. (2009) attributed this difference to possible impedance of the soil heat flux by surface residue. Differences in average monthly DHSVM modeled surface temperature for NT and CT are shown in Figure 13. Differences in the surface energy balance caused by albedo and transmittance through the residue layer resulted in higher average temperatures for NT during the months of November, December, and January,

which led to fewer freezing events. During the rest of the year residue had the opposite effect, making surface temperatures lower in NT than in CT.

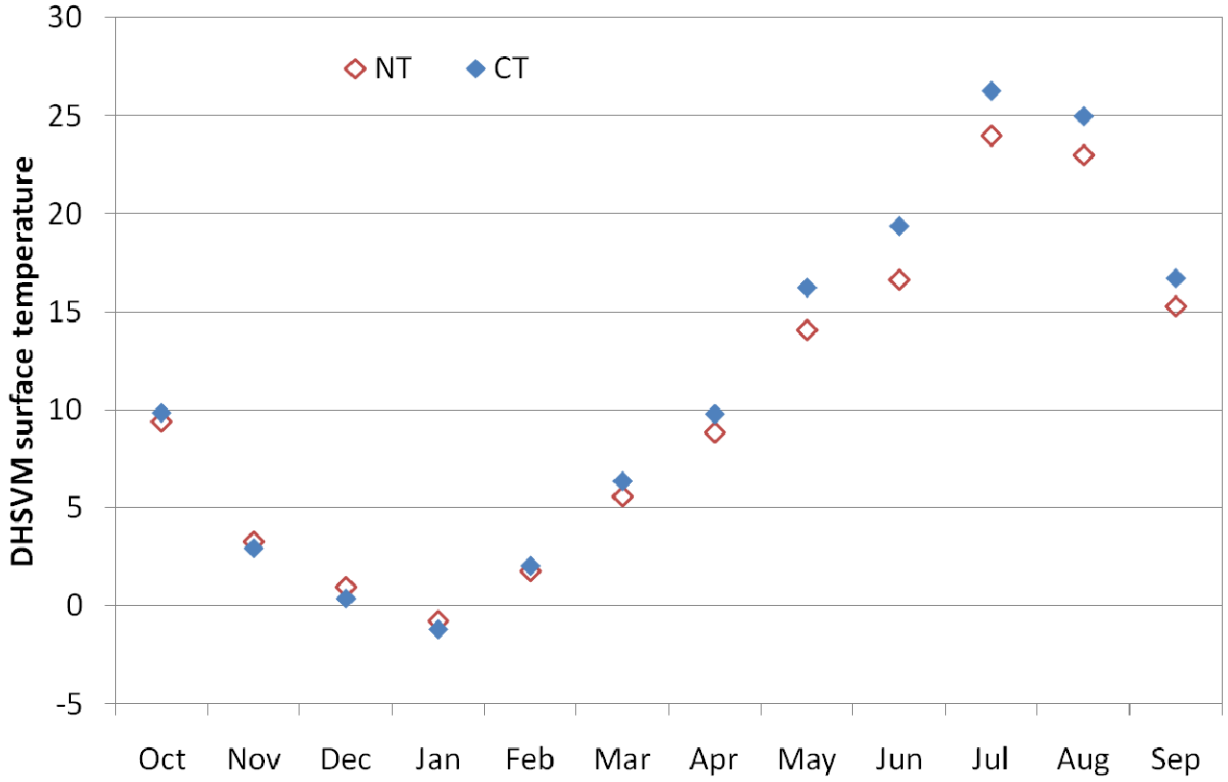

Figure 13. Average DHSVM modeled monthly temperatures for CT and NT during 2004 and 2005.

4. Management scenarios

The effects of the two management scenarios (NT and CT) were examined in the South Fork Basin during the winter season of 2004-2005. The period analyzed began on November 27, 2004 when the first freeze was observed at the PCFS site and ended on April 1, 2005. The basin-wide average volumetric soil moisture content through the winter season is shown in Figure 14 for NT and CT scenarios with and without the effects of frozen soil. Land cover in the South Fork

basin is 82% agriculture, so the impacts of different tillage practices affect the majority of the area.

Water content in the NT scenario was greater than water content in the CT scenario during the entire winter. Average basin volumetric water content decreased from approximately 0.30 to 0.15 during the month of December in the CT scenario; after this there were basin-wide increases in water content during precipitation events, but water content did not increase above 0.30 again until the end of March during a very large rainfall event. Water content in the NT scenario followed a similar trend as the CT scenario, but increases and decreases in soil moisture were less pronounced, with the average basin water content being greater than 0.30 for a majority of the winter. On April 1, average water content for the CT scenario was 0.29, and average water content in the NT scenario was 0.34.

As illustrated in Figure 14, the effect of frozen soil is not the primary cause of differences in water content between CT and NT. The differences are mainly attributed to the effect of modeling NT as an understory vegetation layer and CT as bare ground. Evaporation is the primary process affected by the presence of the understory; Figure 15 depicts average evaporation through the basin for NT and CT scenarios. Only bare soil evaporation is considered in the CT scenario, and the depicted evaporation for the NT scenario includes evaporation from both soil and interception storage. Evaporation from the CT scenario was greater than 3 mm/day at several points during the winter, while NT evaporation was never greater than approximately 0.001 mm/day. The greatest amount of evaporation from NT occurred after precipitation events when water was available from interception and surface storage. NT evaporation consisted of 82% evaporation of intercepted water, with soil evaporation

contributing the remaining 18%. The CT scenario responded similarly, with high amounts of bare soil evaporation following precipitation events, but also had a steady amount of baseline evaporation through most of the winter that was still greater than the largest single evaporation events under NT.

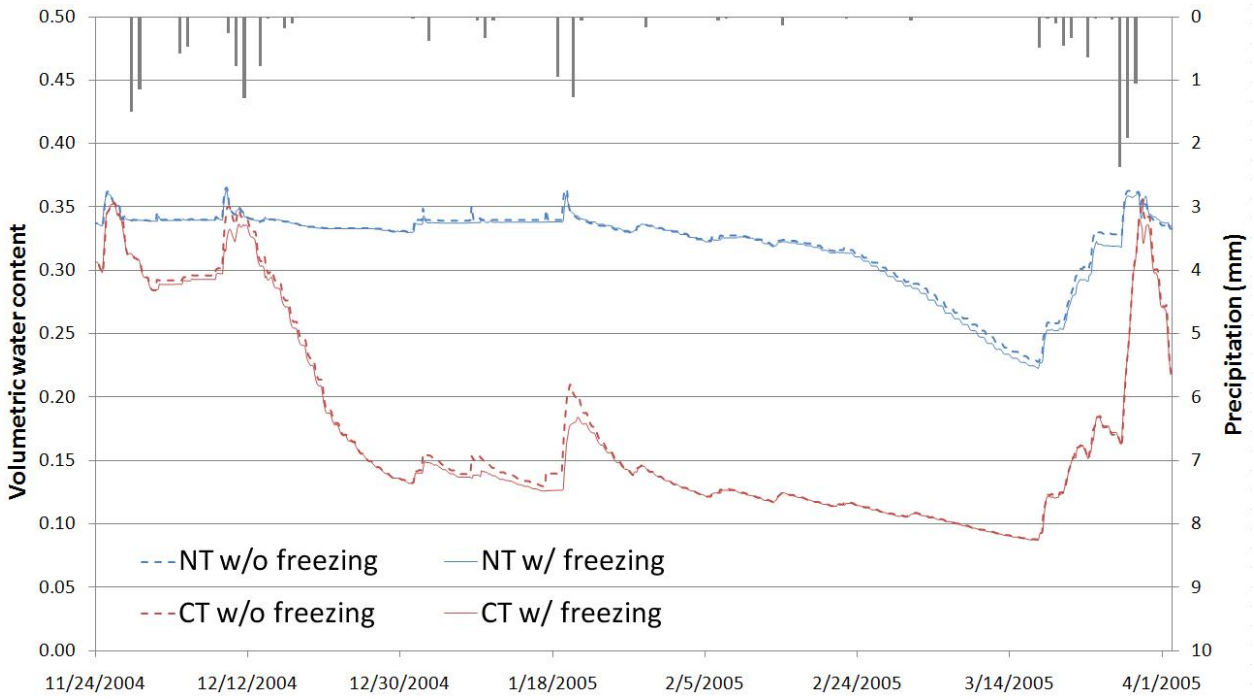

Figure 14. Average daily volumetric water content for NT and CT scenarios with and without reduced infiltration during days with frozen ground.

The CT scenario experienced a larger period of time with frozen soil than the NT scenario. Because DHSVM was run at a 3-hour time-step, there were many days in which several time-steps were predicted to have frozen soil while the average daily surface temperature was greater than 0° C. During the winter of 2004-2005, there were 455 time-steps predicted to be frozen with CT parameters and 405 frozen time-steps with NT parameters based on average soil temperature throughout the basin. By percentage, the ground was frozen

during 45% of the winter with CT and 40% with NT. Soil often became frozen later and thawed earlier when air temperatures were around 0° C with NT than with CT.

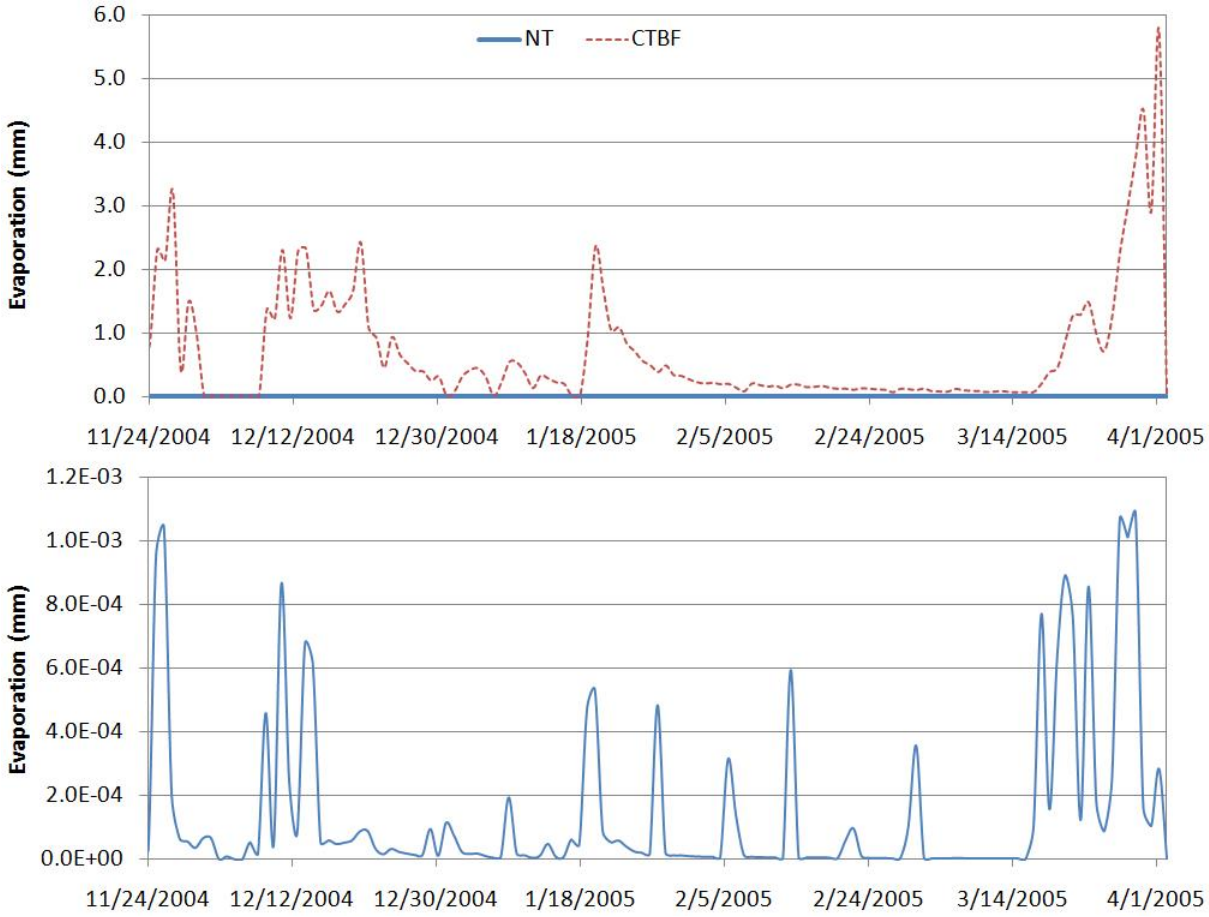

Figure 15. Total daily evaporation from the NT and CT scenarios for the South Fork basin. NT and CT are shown on separate axes so that both can be seen.

The differences in soil moisture on April 1, 2005 due to the combined effects of understory cover and decreased infiltration into frozen ground are shown in Figure 16. The average volumetric soil moisture content was 0.34 in agricultural areas for the NT scenario, while the CT scenario had an average soil moisture content of 0.29. The difference in soil moisture is caused largely by the ability of the residue layer to retain water at the surface by

limiting bare soil evaporation and to a lesser extent is caused by decreased infiltration in the CT scenario due to soil freezing as regulated by transmittance and albedo parameters in the energy balance. Changes in volumetric soil moisture content caused directly by freezing were negligible in both the CT and NT scenarios, being less than 0.01 in both cases. Some pixels can be seen to have a much higher water content than the pixels around them. This may have been caused by inaccuracies in the stream network, as most of the pixels that had significantly higher water contents were located at the end of stream segments where the stream network may need to be extended further so that proper flow routing will occur.

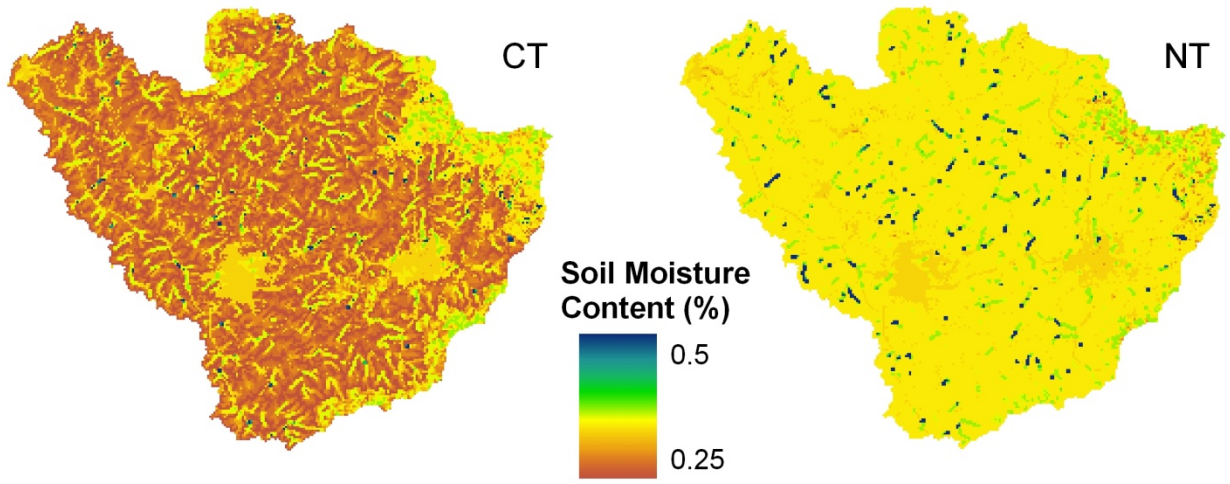

Figure 16. Volumetric soil water in the South Fork Basin caused by modeling CT as bare soil and NT as an understory vegetation layer without transpiration.

DHSVM results indicating that NT management has the ability to retain a higher amount of soil moisture than CT are corroborated by multiple field-scale studies in the Palouse region. Fuentes et al. (2003) found that winter soil moisture was about 0.05 to 0.10 m^3m^{-3} greater in NT than CT, with an average difference of 0.05 during the winter, which agrees with the increase in

water content from 0.29 (CT) to 0.34 (NT). Fuentes et al. also reported that recharge and depletion of soil water were dominated by precipitation and evapotranspiration, while runoff was less consequential. Greer et al. (2006) and Singh et al. (2009), who both performed field studies at the PCFS site, reported a similar increase in soil water content of 0.05 to 0.1 m^2m^{-3} for NT than CT in the upper 10 cm of the soil profile.

Estimated wheat yields based on modeled water contents for NT and CT are listed in Table 11. The higher spring water content in NT resulted in an increase in estimated yield of 980 kg/ha using the Leggett (1959) method and 944 kg/ha using the Schillinger et al. (2008) method, corresponding to a yield increase of 19% in both cases. Soil moisture contents (cm) were calculated from modeled volumetric water contents under the assumptions that wheat roots were able to extract water up to a depth of 1.2 m (Fuentes et al., 2003) and that all water in the soil profile could be used until the wilting point was reached (0.14 m^3m^{-3} for silt loam).

Table 11. Estimated wheat yields for NT and CT managements based on equation 9 (est. yield 1) and equation 10 (est. yield 2). Spring precipitation is the amount of precipitation received during April, May, and June.

	April 1 soil moist. (frac.)	April 1 soil moisture (cm)	Growing season precip (cm)	Spring Precip (cm)	Est. yield 1 (kg/ha)	Est. yield 2 (kg/ha)
NT:	0.20	24.0	15.1	14.0	4230	5050
CT:	0.15	18.0	15.1	14.0	3350	4150

5. Uncertainties

A number of uncertainties must be addressed in order to fully understand the errors involved in this study and the conclusions that may be drawn from the modeling results. While the results of this study agree with repeated studies that have concluded that no-till farming is

beneficial for decreasing runoff and increasing infiltration (Greer et al., 2006; Singh et al., 2009); the interactions between surface residue, soil freeze and thaw cycles, and the surface hydrologic processes of infiltration, evaporation, and runoff are hard to quantify individually and represent in a physically-based model.

One of the primary sources of error in modeling tillage and residue cover is accurately setting parameters for various tillage practices throughout the region being studied. In this work only CT and NT are studied as the extreme cases on the conventional and conservation sides. To more fully understand what the conversion of existing farmland to NT management would look like it would be beneficial to model other types of conservation tillage that are commonly used and affect field hydrology differently than either CT or NT.

Another uncertainty lies in completely understanding field processes. In analyzing field observations from the PCFS site, it is difficult to separate the effects of soil freezing on runoff and infiltration from other effects such as the possibility of the residue capturing and retaining a greater amount of water that would otherwise contribute to runoff on frozen ground. The largest runoff events observed during the winter periods of 2003-2004 through 2006-2007 occurred on the CT plot while frost tube data and soil temperature indicated that the ground was frozen or thawing. However, NT plots did not produce any runoff during these events even when frozen ground was observed on the NT plot. These observations indicate that while frozen soil factors heavily into runoff on CT fields, there may be other factors that control runoff on NT fields.

One of the factors controlling infiltration may be changes to the physical structure of the soil following tillage. Kenny (1990) found that tillage affects soil compaction, and soil

parameters such as porosity and bulk density are adjusted for tillage effects in models such as WEPP (Laflen et al., 1991a, b). To more thoroughly represent and model the impact of tillage on infiltration and runoff, the effect of tillage on soil properties should be considered.

Another uncertainty concerns the way that soil temperature behaves under different tillage practices. Data from the PCFS farm indicate that there is a difference in temperature between NT and CT, but that the difference is not significant, being less than 1° C for all observed periods. Similar results were found by Vomocil et al. (1984) who reported temperature differences of approximately 1.5° C between no-till and bare ground. While these data do support the argument that soil temperature is increased with surface residue, a long-term dataset measuring soil temperature under different tillage practices would be beneficial in more fully understanding the degree to which the residue layer affects soil temperature and freezing in the Palouse region.

Prediction of runoff on frozen soil is further complicated because of the simplified frozen soil model used in DHSVM. Soil freezing is a complex process influenced by factors such as soil structure, initial water content, and local climate but is simplified in this work into an algorithm that take into account heat storage and latent heat effects and predicts only two states; the soil surface is either completely frozen or completely thawed. The difference in soil freezing between CT and NT is often not only in the timing of freezing and thawing, but also in the depth of frost, which can impact the movement of water below the surface. This is evidenced by measurements from the PCFS site and other sites in the Northwest (Pikul et al., 1986; Zuzel et al., 1982) where it was found that frost depth extended to a much greater depth in CT treatments than NT treatments.

Model calibration at two different scales provides another possibility for error. This is apparent particularly in calibration of the c_f value used in equation 2 for reducing the infiltration rate under frozen conditions. The c_f factor was calibrated so that the fraction of runoff to available water from precipitation and SWE would be increased during freezing because of restricted infiltration. However, because the time of runoff and measurement are both uncertain there is error inherently involved in calculating this fraction. This uncertainty carries into basin scale modeling when the c_f factor is applied to predict changes in infiltration due to freezing throughout different areas in the watershed, which are modeled under the additional assumption that these areas will behave similarly to the PCFS field plots, while in reality they may react differently to frozen soils.

Other issues may also factor into the difference between field and basin scale calibrations. Land characteristics on an individual hillslope, such as topography and solar aspect may have dramatic effects on the accumulation, drift, and melt of snow, the dynamics of subsurface flow, and the freezing and thawing of soil. When running the model over an entire watershed these small-scale processes are missed. Because of this it is possible for DHSVM to be well calibrated for a specific field plot, but not well calibrated when scaled up to the entire region, as processes such as infiltration and runoff can be different between the two scales.

CONCLUSION

The purpose of this study was to use DHSVM to analyze the impact of tillage on the winter hydrology of the Palouse region by specifically comparing factors affecting frozen soil infiltration and evaporative water loss under widespread CT and NT management conditions. Differences in winter soil moisture storage and the resulting crop yield estimates were compared between the two management scenarios.

It was found that DHSVM simulations with NT model parameters resulted in a higher root-zone soil moisture content during the winter and spring months. Average volumetric water content in the South Fork basin was 0.32 on average between the months of November and April under NT management, while water content was 0.18 under CT. April 1st soil moisture was 0.29 for CT and 0.34 for NT. This higher soil moisture contributed to an increase in crop yield of 19% when using NT rather than CT according to yield prediction methods developed by Leggett (1959) and Schillinger et al. (2008). Higher yields due to increased availability of water can potentially improve crop production in the Palouse region where wheat growth is typically limited by water. While NT cropping practices may provide some benefits, farmers should also take into account other management factors, such as possible delayed planting times due to excess water in low-lying areas when considering the benefits of switching to an NT system.

The increase in NT soil moisture was attributed primarily to decreased evaporation as a result of the crop residue layer covering the surface. Approximately 90 mm water was evaporated from the South Fork basin with CT, while less than 1 mm was evaporated with NT. To a lesser extent, lower soil temperatures in CT caused more frequent soil freezing that

resulted in decreased evaporation and greater runoff than NT. However, the impact of soil freezing on soil moisture was minimal compared to evaporation.

DHSVM demonstrated the potential for answering pertinent scientific questions using regional-scale modeling of agricultural management practices. Through incorporating a simplified frozen soil model, DHSVM was able to predict surface temperature with a N.S. model efficiency of 0.60, accurately predicting the frozen or unfrozen ground for 81% of winter days. The model surface energy balance was varied for CT and NT through adjusting albedo and transmittance parameters, which allowed unique infiltration and runoff modeling for the two managements and provided a better understanding of the regional impacts of adopting one of the practices. DHSVM has the potential to be used in further development of regional tillage modeling, and may also be applied for the investigation of the various other factors that contribute to regional issues such as crop yield, sustainable farming, and future management decisions.

To more thoroughly understand the impacts of NT farming, further attention should be given to understanding the individual processes affected by tillage. Water retention in the mass of surface crop residue and tillage effects on soil compaction should be considered. Modeling in DHSVM can be improved by incorporating a more complete frozen soil model that includes the advance and retreat of frost beneath the surface and that is informed by a more comprehensive historical dataset of freezing as a function of different managements. Additionally, more scenarios should be explored to understand the effects that the wide range of conservation tillage strategies have on over-winter soil moisture.

Future directions include modeling crop growth dynamics to more accurately study the effects of tillage and investigating the significance of tillage in an altered climate. By coupling DHSVM with a crop growth model such as CropSyst (Stockle et al., 2003) it would be possible to create a model for hydrology and vegetation that could be used for a more thorough study on the impacts of tillage on water availability for the crop growth cycle and the corresponding crop yield. In a semi-arid region such as the Palouse it is also necessary to understand possible climate change scenarios and their impact on the future of regional farming. Because tillage is an important aspect of farming with potentially large impacts on regional hydrology, it will be important to understand how tillage will factor into the best possible management of fields under possible climate change situations.

REFERENCES

Alberts, E. E., M. A Nearing, M. A. Weltz, L. M. Risse, F. B. Pierson, X. C. Zhang. J. M. Laflen, and J. R. Simanton (1995), USDA-Water Erosion Prediction Project hillslope profile and watershed model documentation, NSERL Report #10.

Andreadis, K., P. Storck, and D. P. Lettenmaier (2009), Modeling snow accumulation and ablation processes in forested environments, Water Resources Research, 45.

Arnold, J. G., and N. Fohrer (2005), SWAT2000: current capabilities and research opportunities in applied watershed modeling, Hydrological Processes, 19, 563-572.

Beckers, J., and Y. Alila (2004), A model of rapid preferential hillslope runoff contributions to peak flow generation in a temperate rain forest watershed, Water Resources Research, 40 (doi:10.1029/2003WR002582).

Breuer, L., K. Eckhardt, and H.-G. Frede (2003), Plant parameter values for models in temperate climates, Ecological Modeling, 169, 237-293.

Chan, K. Y., and D. P. Heenan (1996), Effect of tillage and stubble management on soil water storage, crop growth and yield in a wheat-lupin rotation in southern NSW, Aust. J. Agric. Res., 47, 479-488.

Chow, V. T., D. R. Maidmont, and L. W. Mays (1988), Applied Hydrology, McGraw-Hill, Singapore.

Chu, S. T. (1978), Infiltration during an unsteady rain, Water Resources Research, 14(3), 461-466.

Cochran, V. L., L. F. Elliot, and R. I. Papendick (1982), Effect of crop residue management and tillage on water use efficiency and yield of winter wheat, Agronomy Journal, 74(6), 929-932.

Cornish, P. S., and J. E. Pratley (1991), Tillage practices in sustainable farming systems, in Dryland Farming: A Systems Approach, edited by V. Squires and P. Tow, pp. 76-101, Sydney University Press, Melbourne, Australia.

Cuo, L., D. P. Lettenmaier, M. Alberti, and J. E. Richey (2009), Effects of a century of land cover and climate change on the hydrology of the Puget Sound basin, Hydrological Processes, 23, 907-933.

Daly, C., R.P. Neilson, and D. L. Phillips (1994), A statistical-topographic model for mapping

climatological precipitation over mountainous terrain, Journal of Applied Meteorology, 33, 140-158.

Davis, D. J., and M. Molnau (1973), The water cycle on a watershed in the Palouse region of Idaho, Trans. ASAE, 15, 178-589.

Day, A. D., and S. Intalap (1970), Some effects of soil moisture stress on growth of wheat, Agronomy Journal, 62, 27-29.

Dingman, S. L. (1994), Physical Hydrology, Macmillan, New York.

Doten, C. O., L. C. Bowling, Lanani, J. S., Maurer, E. P., Lettenmaier, D. P. (2006), A spatially distributed model for the dynamic prediction of sediment erosion and transport in mountainous forested watersheds, Water Resources Research, 42 (doi:10.1029/2004WR003829).

Dowding, E. A., K. N. Hawley, and C. L. Peterson (1984), Characterization of runoff as related to tillage management, in 1984 Winter Meeting of the American Society of Agricultural Engineers, edited, ASAE.

Elsner, M. M., L. Cuo, N. Voisin, J. S. Deems, A. F. Hamlet, J. A. Vano, K. E. B. Mickelson, S.-Y. Lee, and D. P. Lettenmaier (2009), Implications of 21st century climate change for the hydrology of Washington State, Climatic Change (doi:10.1007/s10584-010-9855-0).

Farr, T. G. (2007), The shuttle radar topography mission, Reviews of Geophysics, 45.

Fuentes, J. P., M. Flury, D. R. Huggins, and D. F. Bezdicek (2003), Soil water and nitrogen dynamics in dryland cropping systems of Washington State, USA, Soil & Tillage Research, 71, 33-47.

Greer, C. R., J. Q. Wu, P. Singh, and D. K. McCool (2006), WEPP Simulation of observed winter runoff and erosion in the U.S. Pacific Northwest, Vadose Zone Journal, 5, 261-272.

Guy, S. O., D. B. Cox (2002), Reduced tillage increases fesidue groundcover in subsequent dry pea and winter wheat crops in the Palouse region of Idaho, Soil and Tillage Research, 66, 69-77.

Hamlet, A.F., and D. P. Lettenmaier (2005), Production of temporally consistent gridded precipitation and temperature fields for the continental United States. Journal of Hydrometeorology, 35, 1597-1624.

Hammel, J. E. (1996), Water conservation practices for sustainable dryland farming systems in the Pacific Northwest, Am. J. Alternative Agric., 11, 58-63.

Hammel, J. E., R. I. Papendick, and G. S. Campbell (1981), Fallow tillage effects on evaporation and seedzone water content in a dry summer climate, Soil Sci. Soc. Am. J., 45, 1016-1022.

Hanks, R. J., and F. C. Thorp (1956), Seedling emergence of wheat as related to soil moisture content, bulk density, oxygen diffusion rate, and crust strength, Soil Science Society Proceedings, 307-310.

Hershfield, D. M. (1974), Frequency of freeze-thaw cycles, J. Appl. Meterol., 13, 348-354.

Homer, C., C. Huang, L. Yang, B. Wylie, and M. Coan (2004), Development of a 2001 national land-cover database for the United States, Photogrammetric Engineering & Remote Sensing, 70(7), 829-840.

Inagaki, M. N., J. Valkoun, and M. M. Nachit (2007), Effect of soil water deficit on grain yield in synthetic bread wheat derivatives, Cereal Research Communications, 35(4), 1603-1608.

Jalota, S. K., V. K. Arora, and O. Singh (2000), Development and evaluation of a soil water evaporation model to assess the effects of soil texture, tillage and crop residue management under field conditions, Soil Use and Management, 16, 194-199.

Juergens, L. A., D. L. Young, W. F. Schillinger, and H. R. Hinman (2004), Economics of alternative no-till spring crop rotations in Washington's wheat-fallow region, Agron. J., 96, 154-158.

Kenny, J. F. (1990), Measurement and prediction of tillage effects on hydraulic and thermal properties of palouse silt loam soil, Washington State Univ., Pullman.

Laflen, J. M., L. J. Lane, and G. R. Foster (1991), WEPP: A new generation of erosion prediction technology, Journal of Soil and Water Conservation, 46, 30-34.

Laflen, J. M., W. J. Elliot, J. R. Simanton, C. S. Holzhey, and K. D. Kohl (1991), WEPP soil erodibility experiments for rangeland and cropland soils, Journal of Soil and Water Conservation, 46, 39-44.

Lal, R., D. C. Reicosky, and J. D. Hanson (2007), Evolution of the plow over 10,000 years and the rationale for no-till farming, Soil Tillage and Research, 93, 1-12.

Lane, L. J., M. H. Nichols, and G. B. Paige (1995a), Modeling erosion on hillslopes: concepts, theory and data, Proc. Int. Congress on Modelnig and Simulation, P. Binning, H. Bridgeman, and B. Williams, eds., 1-7.

Lane, L. J., M. H. Nichols, and J. R. Simanton (1995b), Spatial variability of cover affecting erosion and sediment yield in overland flow, in Effects of scale on interpretation and

management of sediment and water quality, Proc., Boulder Symp., W. R. Osterkamp, ed., Int. Assoc. Hydrol. Pub. No. 226, 147-152.

Leggett, G. E. (1959), Relationships between winter wheat yield, available moisture and nitrogen in eastern Washington dryland areas, Washington Agricultural Experimental Station Bulletin 609, 1-16.

Lindstrom, M. J., R. I. Papendick, and F. E. Koehler (1976), A model to predict winter wheat emergence as affected by soil temperature, water potential, and depth of planting, Agronomy Journal, 68, 137-141.

Maidmont, D. R. (1992), Handbook of Hydrology, McGraw-Hill, New York.

Maurer, E. P., A. W. Wood, J. C. Adam, and D. P. Lettenmaier (2002) A long-term hydrologically based dataset of land surface fluxes and states for the conterminous United States, Journal of Climate, 15, 3237-3251.

McCool, D. K., and R. D. Roe (2005), Long-term erosion trends on cropland in the Pacific Northwest, edited, ASAE, St. Joseph, Mich.

McCool, D. K., K. E. Saxton, and P. K. Kalita (2006), Winter runoff and erosion on Northwestern USA cropland, in 2006 ASABE Annual International Meeting, edited, ASABE, St. Joseph, Mich, Portland, Oregon.

Mitchell, K. E. (2004), The multi-institutional North American Land Data Assimilation System (NLDAS): utilizing multiple GCIP products and partners in a continental distributed hydrological modeling system, Journal of Geophysical Research, 109.

Mizuba, M. M., and J. E. Hammel (2001), Infiltration rates in fall-seeded winter wheat fields following preplant subsoil tillage, Journal of Soil and Water Conservation, 56(2), 133-137.

Nash, J. E., and Sutcliffe, J. V. (1970), River flow forecasting through conceptual models. Part 1 - a discussion of principles, Journal of Hydrology, 10, 282-290.

NCDC (National Climatic Data Center), 2009. http://www.ncdc.noaa.gov/oa/ncdc.html, accessed on February 13, 2009.

NFWA (North Fork Coeur d'Alene River Watershed Assesment), Watershed Professionals Network, February, 2007

Noori, F., F. E. Bolton, and D. N. Moss (1985), Water injection at seeding of winter wheat, Agronomy Journal, 77, 906-908.

Novak, M. D., W. Chen, and M. A. Hares (2000), Simulating the radiation distribution within a barley-straw mulch, Agricultural and Forest Meteorology, 102, 173-186.

Ochsner, T. E., R. Horton, and T. Ren (2001), A new perspective on soil thermal properties, Soil Science Society of America Journal, 65, 1641-1647.

Oweis, T., M. Pala, and J. Ryan (1999), Management alternatives for improved durum wheat production under supplemental irrigation in Syria, European Journal of Agronomy, 11, 255-266.

Owen, P. C. (1952), The relation of germination of wheat to water potential, Journal of Experimental Botany, 3, 188-203

Pannkuk, C. D., C. O. Stockle, and R. I. Papendick (1998), Evaluation CropSyst simulations of wheat management in a wheat-fallow region of the US Pacific Northwest, Agricultural Systems, 57(2), 121-134.

Papendick, R. I., and D. K. McCool (1996), Farming systems and conservation needs in the Pacific Northwest wheat region, Am. J. Alternative Agric., 11, 52-57.

Pikul, J. L., J. F. Zuzel, and R. N. Greenwalt (1986), Formation of soil frost as influenced by tillage and residue management, Journal of Soil and Water Conservation, 41(3), 196-199.

Pikul, J. L., D. E. Wilkins, J. K. Aase, and J. F. Zuzel (1996), Contour ripping: A tillage strategy to improve water infiltration into frozen soil, Journal of Soil and Water Conservation, 51(1), 76-83.

PRISM Group, Oregon State University, http://www.prismclimate.org, created 10 April 2009.

Saxton, K. E., W.J. Rawls, J. S. Romberger, and R. I. Papendick (1986), Estimating generalized soil-water characteristics from texture, Soil Science Society of America Journal, 50, 1031-1036.

Schillinger, W. F., and F. E. Bolton (1993), Fallow water storage in tilled vs. untilled soils in the Pacific Northwest, J. Prod. Agric., 6(2), 267-269.

Schillinger, W. F., A. C. Kennedy, and D. L. Young (2007), Eight years of annual no-till cropping in Washington's winter wheat-summer fallow region, Agriculture, Ecosystems and Environment, 120, 345-358.

Schillinger, W. F., S. E. Schofstoll, J. R. Alldredge (2008), Available water and wheat grain yield relations in a Mediterranean climate, Field Crops Research, 109, 45-49.

Singh, P., J. Q. Wu, D. K. McCool, S. Dun, C.-H. Lin, and J. R. Morse (2009), Winter hydrologic and

erosion processes in the U.S. Palouse region: field experimentation and WEPP simulation, Vadose Zone Journal, 8(2), 426-436.

Singh, V. P., and D. A. Woolhiser (2002), Mathematical modeling of watershed hydrology, Journal of Hydrologic Engineering, 7(4), 270-292.

Stockle, C. O., M. Donatelli, R. Nelson (2003), CropSyst, a cropping systems simulation model, European Journal of Agronomy, 18, 289-307.

Storck, P., L. Bowling, P. Wetherbee, and D. Lettenmaier (1998), Application of a GIS-based distributed hydrology model for prediction of forest harvest effects on peak stream flow in the Pacific Northwest, Hydrological Processes, 12, 889-904.

Thornton, P. E., and S. W. Running (1999), An improved algorithm for estimating incident daily solar radiation from measurements of temperature, humidity, and precipitation, Agricultural and Forest Meteorology, 93, 211-228.

Thyers, M., J. Beckers, D. Spittlehouse, Y. Alila, and R. Winkler (2004), Diagnosing a distributed hydrologic model for two high-elevation forested catchments based on detailed stand- and basin-scale data, Water Resources Research, 40 (doi:10.1029/2003WR002414).

Tomer, M. D., C. A. Cambardella, D. E. James, T. B. Moorman (2006), Surface-soil properties and water contents across two watersheds win contrasting tillage histories, Soil Science Society of America Journal, 70, 620-230.

Tomer, M. D., D. W. Meek, L. A. Kramer (2005), Agricultural practices influence flow regimes of headwater streams in Western Iowa, Journal of Environmental Quality, 34, 1547-1558.

USDA-NRCS (U.S. Department of Agriculture-Natural Resources Conservation Service), 2009, Soil Survery Geographic (SSURGO) Database. http://www.ncrs.usda.gov/products/datasets/ssurgo/index.html, accessed on February 13, 2009.

USDA-NRCS (U.S. Department of Agriculture-Natural Resources Conservation Service), 2010, What is snow water equivalent? http://www.or.nrcs.usda.gov/snow/about/swe.html#top, accessed on June 22, 2009.

Vomocil, J. A., J. L. Zuzel, R. E. McDole, and C. F. Engle (1984), Stubble management influences soil freezingRep., Oregon State University Ext. Serv.

Whitaker, A., Y. Alila, J. Beckers, and D. Toews (2003), Application of the Distributed Soil Hydrology Vegetation Model to Redfish Creek, British Columbia: model evaluation using internal catchment data, Hydrological Processes, 17, 199-224.

Wigmosta, M. S., and S. J. Burges (1997), An adaptive modeling and monitoring approach to describe the hydrologic behavior of small catchments, J. Hydrol, 202, 48-77.

Wigmosta, M. S., V. L. W., and D. P. Lettenmaier (1994), A distributed hydrology-vegetation model for complex terrain, Water resources research, 30(6), 1665-1679.

Wigmosta, M. S., L. J. Lane, J. D. Tagestad, and A. M. Coleman (2009), Hydrologic and erosion models to assess land use and management practices affecting soil erosion, Journal of Hydrologic Engineering, 14(1), 27-41.

Wise, E. K., and A. C. Comrie (2006), Extending the Kolmogorov-Zurbenko filter: application to ozone, particulate matter, and meteorological trends, J. Air & Waste Manage. Asooc., 55, 1208-1216.

Zuzel, J. F., R. R. Allmaras, and R. Greenwalt (1982), Runoff and soil erosion on frozen soils in northeastern Oregon, Journal of Soil and Water Conservation, 37(6), 351-354.